50 Jahre
1956 - 2006

GKSS
FORSCHUNGSZENTRUM
in der HELMHOLTZ-GEMEINSCHAFT

The Use of Long-Term Observations in Combination with Modeling and Their Effect on the Estimation of the North Sea Storm Surge Climate

(Vom Fachbereich Geowissenschaften der Universität Hamburg als Dissertation angenommene Arbeit)

Author:

T. Aspelien

ISSN 0344-9629

HELMHOLTZ GEMEINSCHAFT

GKSS ist Mitglied der Helmholtz-Gemeinschaft Deutscher Forschungszentren e.V.

wissen schafft nutzen

GKSS 2006/2

GKSS 2006/2

The Use of Long-Term Observations in Combination with Modeling and Their Effect on the Estimation of the North Sea Storm Surge Climate

(Vom Fachbereich Geowissenschaften der Universität Hamburg als Dissertation angenommene Arbeit)

Author:
T. Aspelien
(Institute for Coastal Research)

GKSS-Forschungszentrum Geesthacht GmbH • Geesthacht • 2006

Die Berichte der GKSS werden kostenlos abgegeben.
The delivery of the GKSS reports is free of charge.

Anforderungen/Requests:

GKSS-Forschungszentrum Geesthacht GmbH
Bibliothek/Library
Postfach 11 60
D-21494 Geesthacht
Germany
Fax.: (49) 04152/871717

ISSN 0344-9629

GKSS-Forschungszentrum Geesthacht GmbH · Telefon (04152)87-0
Max-Planck-Straße 1 · D-21502 Geesthacht / Postfach 11 60 · D-21494 Geesthacht

GKSS 2006/2

The Use of Long-Term Observations in Combination with Modeling and Their Effect on the Estimation of the North Sea Storm Surge Climate

(Vom Fachbereich Geowissenschaften der Universität Hamburg als Dissertation angenommene Arbeit)

Trygve Aspelien

106 pages with 30 figures and 5 tables

Abstract

The aim of this PhD thesis is to design, implement and assess a method to combine long-term observations with multi-decadal model simulations. In this work a computationally cost-efficient nudging method, well suited for multi-decadal simulations, is chosen.

First, the nudging method was tested for its sensitivity to different parameters. Then the long-term observations of sea level height from the UK tide gauge Aberdeen were combined with a multi-decadal hindcast for the North Sea. Compared to a control simulation, in which no observed values of sea level height were combined with the model, the nudging method generally improves the modeled water levels with respect to the observed values, especially for surge.

The estimation of long-term fluctuations and biases of extreme values of high waters in the nudged simulation are generally considerably improved after nudging and closer to the observed. The effect is largest in the German Bight and at the West coast of Denmark.

It is concluded that the cost-efficient nudging method, in which external processes, such as external surges, are additionally taken into account, provides a considerable improvement in reproducing long-term variations and trends, especially for surge. Without additional data from e.g. observed values from tide gauges taken into account, the meteorological induced long-term variations in a hindcast are not fully captured.

Der Einfluss von Langzeit-Beobachtungen bei der Modellierung des Windstauklimas der Nordsee

Zusammenfassung

Ziel dieser Doktorarbeit ist es, eine Methode zu entwerfen, zu implementieren und zu bewerten, um langfristige Beobachtungen mit langen Modellsimulationen über mehrere Jahrzehnte zu kombinieren. Es wird eine Nudging-Methode gewählt, die wenig zusätzliche Rechenzeit erfordert und damit für diese Art von Simulationen gut geeignet erscheint.

Die Nudging-Methode wurde zuerst hinsichtlich ihrer Sensitivität bezüglich der Variation verschiedener Parametern untersucht. Anschließend wurden langfristige Beobachtungen des Wasserstandes vom britischen Pegel Aberdeen mit einem langen Hindcast über mehrere Jahrzehnte für die Nordsee kombiniert. Verglichen mit einem Kontrolllauf, in dem keine beobachteten Pegelwerte des Wasserstandes mit dem Modell kombiniert wurden, verbessert das Nudging die modellierten Wasserstände in Bezug auf beobachtete Werte (insbesondere für Windstau).

Die Schätzung der langfristigen Fluktuationen und die Fehler der extremen Werte des Hochwassers werden im Allgemeinen in der Simulation mit Nudging beträchtlich verbessert. Die Auswirkung des Nudgings ist in der Deutschen Bucht und an der Westküste Dänemarks am größten.

Die Nudging-Methode, in der externe Prozesse wie z.B. Fernwellen zusätzlich in Betracht gezogen werden, stellt eine beträchtliche Verbesserung dar, wenn man langfristige Veränderungen und Tendenzen, besonders für Windstau, untersucht. Ohne zusätzliche Daten von z.B. beobachteten Pegelwerten wird die meteorologisch verursachte langfristige Variabilität des Hindcasts nicht völlig beschrieben.

Manuscript received / Manuskripteingang in TDB: 15. März 2006

Contents

Summary

The aim of this PhD thesis is to design, implement and assess a method to combine long-term observations with multi-decadal model simulations. Information about long-term behavior is needed for e.g., assessment of long-term variability, as a background against which climate changes have to be assessed, or for extreme value analysis used for coastal construction works such as e.g., storm-surge barriers. The intention is to use the designed method to combine observed sea level height with the model to get an improved, homogeneous and higher resolved description of the extreme water levels and trends in the North Sea for the time period 1958-2001.

Ocean sciences today use a large variety of different methods to combine observations with models. An important criterion for choosing a suitable method for multi-decadal data-driven simulations is extra computing time, and in this work a nudging method is chosen. The nudging is performed in the regional ocean model TRIMGEO.

The nudging method was tested for its sensitivity to different parameters. Long-term observations of sea level height from the UK tide gauge Aberdeen were combined with a multi-decadal hindcast for the North Sea and compared to a control simulation. Both simulations were driven by identical sea level pressure and near-surface wind fields obtained from a regional multi-decadal atmospheric reconstruction. Additional improvement from combining observations from more UK tide gauges was negligible for the German Bight, which was the main area of interest.

The results from the nudged hindcast is systematically investigated and compared to long-term observations for selected tide gauges. The root-mean-square error of modeled sea level height was reduced by 30-60% for tide gauges in the German Bight and in Norway when observed water levels for Aberdeen were combined with the model. For surge, a considerable reduction of 70-80% was achieved for the German Bight.

The estimation of long-term fluctuations and biases of extreme values of high waters in the nudged simulation are generally considerably improved after nudging, however, this improvement is at the cost of a higher bias in the description of low waters. For surge, a clear improvement is achieved from nudging. The closer investigated tide gauges in the German Bight improve by 10%-80% for the high an low percentiles in the experiment with nudging applied, compared to the control simulation. The trends for the 95th percentile calculated from surge in the experiment with nudging applied are significantly different from the trends from the experiment without nudging

for most parts of the North Sea. The largest differences are seen in the German Bight and at the West coast of Denmark. In this area positive trends of 15-30 cm/100 years are calculated for the experiment with nudging applied.

It is concluded that the cost-efficient nudging method, in which external processes, such as external surges, are additionally taken into account, provides a considerable improvement in reproducing long-term variations and trends, especially for surge. Without additional data from e.g. observed values from tide gauges taken into account, the meteorological induced long-term variations in a hindcast are not fully captured. Furthermore, it is possible to quantify changes in the long-term variations caused by non-meteorological effects from the remaining differences between the experiment with nudging applied and the observations. Such effects could be changes in the bathymetry by e.g. construction works (e.g. dredging, embankments) or natural morphodynamical processes, a rise in mean sea level or land rising/sinking. The method is also a good alternative to extra Atlantic models calculating the boundary conditions or as an option to compensate possible deficiencies in the boundary conditions.

Chapter 1

Introduction

Along the North Sea coast much of the hinterland is below or slightly above mean sea level and has to be protected from extreme events. The Dutch coast line and land areas around the German Bight are especially vulnerable. For example, the West coast of Schleswig-Holstein in is Germany comprised of about 553 km of coastline which is protected by 408 km of dikes (Ministerium für ländliche Räume, Landesplanung, Landwirtschaft und Tourismus des Landes Schleswig Holstein, 2001).

Long-term observations are important for many purposes. Examples are extreme value analysis to be used for construction works or coastal protection, for assessment of long-term variability and as a background which climate change have to be assessed against. A comprehensive study of long-term timeseries by Woodworth and Blackman (2002), analyzed changes in extreme high waters in Liverpool since 1768. Considering the entire period they found considerable inter-annual variability but no clear trend. Another study by von Storch and Reichardt (1997) investigated, among other things, the observed values of high waters from the German tide gauge at Cuxhaven from 1876 to 1993 and found a significant upward trend of 30 cm/ 100 years.

While the analysis of long-term records of tide gauges may reveal the long-term variations at the respective sites, there are many locations where no measurements have been made or where the observational records are too short to allow for the investigation of long-term changes. In these cases, multi-decadal hindcasts performed with numerical models represent an alternative method that complements the analysis of observational records.

One of the first multi-decadal simulations, for a 40 year period, was conducted by Flather et al. (1998). They forced a two-dimensional storm surge model covering the Northwest European continental shelf with meteorological data from the Norwegian Meteorological Institute for the period 1955-1994. Comparing observed and modeled data they concluded that realistic estimates of surge extremes could be derived directly from model simulations, provided that the atmospheric forcing has sufficient quality. They suggested that such estimates could be made for areas (e.g., offshore) or situations (e.g., future climate driven by a constructed atmospheric forcing) where no observational data exist.

Several multi-decadal simulations have already been performed for the North Sea. Kauker and Langenberg (2000) used two ocean models and compared them with respect to their performance in the assessment of sea level change in a changing climate. Both models agreed well and predicted an increase of up to 30 cm of winter mean sea levels when a doubling of CO_2 was applied in the models. Lowe et al. (2001) investigated changes in occurrences of storm surges around the United Kingdom as a potential consequence of climate change. They found a rise in mean sea level and also a reduction in return periods of extreme storm surge events for most of the sites investigated. (e.g., Schrumm 2001) investigated the regionalization of climate change for the North Sea. Furthermore, Flather and Smith (1998) and Lowe et al. (2001) suggested that in combination with climate change scenarios, the natural climate variability obtained from multi-decadal simulations represents an essential backbone for climate change attribution and detection studies.

Wakelin et al. (2003) investigated the connection between changes in the North Atlantic Oscillation (NAO) and the sea level over the Northwest European continental shelf for the period 1955-2000 using a two-dimensional model of tides and storm surges. They found a clear spatial pattern in the correlation between the winter-mean values of sea level and NAO and strongest sensitivity of the sea level to NAO in the southern North Sea.

Langenberg et al. (1999) provided one of the first comprehensive analysis of the storm surge climate for the last decades in the North Sea. They studied trends in storm-related sea level variations along the North Sea Coast obtained from both a hindcast study 1955-1993 and a statistical analysis of observational data and concluded that during the hindcast period winter means of high water levels along the North Sea coast have increased in the order of 1-2 mm/yr. However, the study suffered from a decisive drawback in the homogeneity of the atmospheric forcing and the relative coarse spatial resolution near the coast which prevented the model from reasonably simulating the highest water levels.

An improved storm surge hindcast was subsequently conducted by Weisse and Plüß (2005) in which these drawbacks were reduced and the analysis period was slightly extended. They presented an update of the analysis performed by Langenberg et al. (1999) and investigated the long-term storm surge variability in comparison to that of the earlier hindcast. A high resolution regional ocean model was used, and observational data from Aberdeen were combined with model data. However, Weisse and Plüß (2005) did not, in a systematic way, investigate the sensitivity of simulations deriving from the parameterization of such a method to combine observations with a regional ocean model. Additionally, the effect of the method on extremes and their long-term variations and trends was not systematically investigated and compared with observations. This thesis addresses these weaknesses.

In a strategy paper addressing the coastal module of the global ocean observing system (UNESCO, 2003) it was suggested shortcomings of a numerical model could be reduced by combining existing observations with model hindcasts. The objective of such exercises is not only to yield an improved representation of the observed natural variability but also to provide information about variables that have either not been observed directly or that have been insufficiently sampled in space and time. Even for the most frequent observed values, such as sea surface temperature (SST) shown in Fig. 1.1, there exist vast areas with scarce data coverage. Contrary, while a numerical model, have a good data coverage, the modeled values may be of less quality than the observed data. In this thesis a method is sought to combine observational data with model data for multi-decadal simulations. The last part of this chapter focuses on the background of developing such methods and outlines a strategy for a method suitable for multi-decadal simulations.

The ways of combining observations with models has undergone a rapid development since computers were first introduced and modeling became possible. As the weather has always interested mankind, most of the earliest investigations of observations and modeling tended to focus on the atmosphere. In the first half of the nineteenth century, prior to the computer age, attempts were made to represent meteorological observations on maps and charts. From these maps it was hoped to deduce the governing laws of the atmosphere, and also to be able to make a prognosis of the future state. Synoptic charts were developed in the 1850's and could be used as a basis for prognosis. Everything was carried out by hand, and an objective method was needed.

Bjerknes (1911) proposed that weather was an initial value problem, which could be prognosed by using the governing equations for the atmosphere. Eleven years later, Richardson (1922) made his famous attempt to integrate

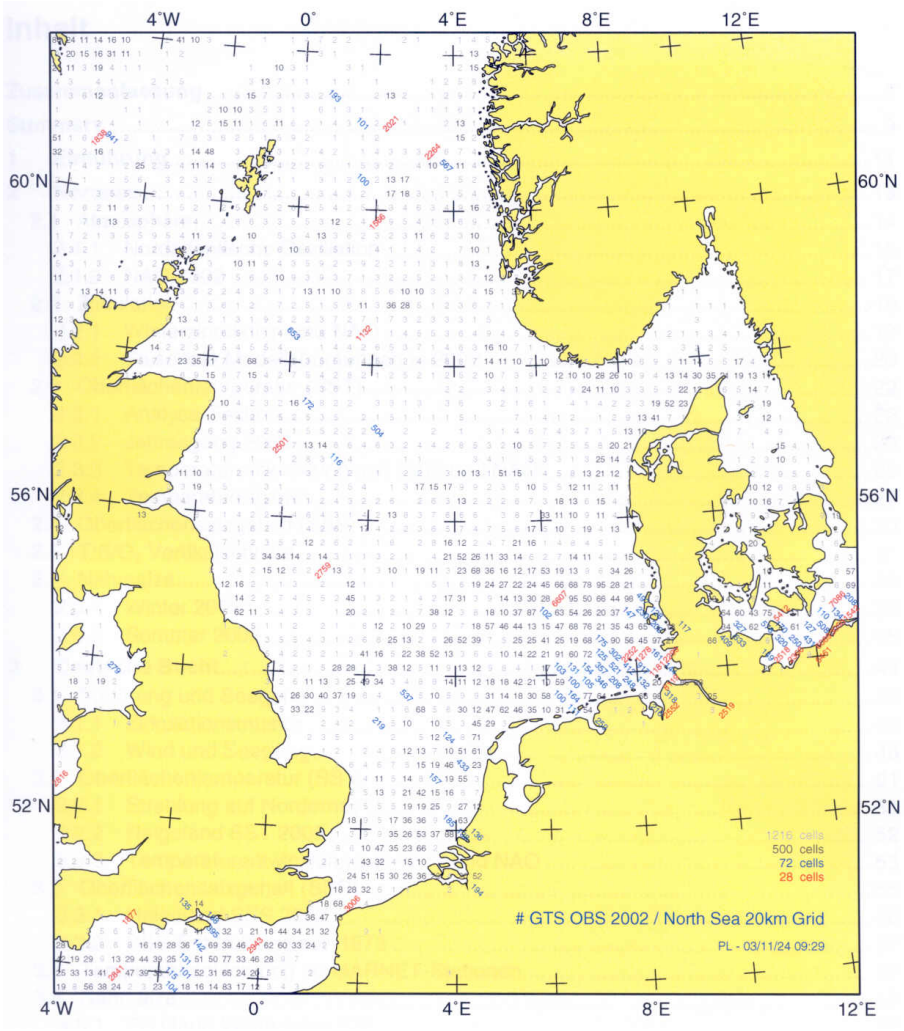

Figure 1.1: Frequency distribution of sea surface temperature (SST) reports in 2002 from World Meteorological Organization's (WMO) Global Telecommunication System (GTS). Even though SST is the best-observed ocean state parameter there are vast areas (about 70% of the entire domain) of scarce data coverage (< 10 observations, gray) off the shipping routes. Most "high frequency" stations (>999 observations, red) belong to the UK's MAWS (Marine Automatic Weather Station) network and the BSH's (German Federal Maritime and Hydrographic Agency) MARNET (Marines Umweltmessnetz in Nord- und Ostsee des BSH). From Loewe et al. (2003), reprinted with permission from BSH.

the discretized governing equations forward in time for Central Europe. Daley (1991) states that this failed for several reasons. One of the reasons was

that the concept of initialization was not understood at that time. Motivated by the first multipurpose digital computer ENIAC [1] at the Princeton Institute for Advanced Study, Charney, Fjortoft and von Neumann in 1950 tried a second attempt (Charney et al., 1950). By using the barotopic vorticity equation, they could successfully prognose atmospheric movements on synoptic scale. However, the method of using subjective analysis was more time consuming than the forecast itself. An automatic procedure was needed to create the initial state values on a dicretisized grid, based on observations irregular in time and space. Using such an automatic method to combine observations with the model was called *objective analysis* because it did not need judgement of a human analyst.

Gilchrist and Cressman (1954) took the idea of an objective analysis a step further, when they fitted polynomials to a local region around an observation, which they called the area of influence. Further, they introduced the concept that an analysis could be improved if a preliminary estimate of the analysis existed. This estimate is now called *background field*, *first guess field* or *prior estimate* (Daley, 1991). Bergthorsson and Doos (1955) advanced this procedure further by introducing an analysis method known as *successive corrections*. From each observation the procedure subtracted a background field obtained from climatology or a previous forecast. These increments were analyzed and later added to the background field. At this time numerical models were common in the science of meteorology, and this objective analysis was the start of combining observations with models and what we today often call *data assimilation*.

In the 1970's numerical primitive equation models were developed, which described the atmosphere using a more general form of the governing equations but at the same time permitting inertia-gravity oscillations with very short time scales. If the model is not in a balanced state between mass and wind fields, large-amplitude spurious inertia-gravity waves can be created in the model. Such waves are unwanted at the start of model simulations as they are an artificial effect of unbalanced initial conditions of the mass and wind fields in the model. This balancing process is called *initialization* and is necessary for all numerical models based on primitive equations. The concept of initialization is one important part of the *data assimilation cycle* described by Daley (1991) as a cycle involving the following four components:

1. Quality Control
2. Objective analysis

[1] Electronic Numerical Integrator And Computer

3. Initialization
4. Short forecast to prepare the next background field.

Today it is more common to use the term *data assimilation* for techniques that effectively combine dynamical models with observational data. Brink and Robinson (1998) define a data assimilation system as a system consisting of three components: a set of observations, a dynamical model and a data assimilation scheme or melding scheme. A set of measurements has errors arising from various sources. On one hand it will be subject to errors arising from e.g., instrumental noise, sampling and the interpretation of sensor measurements as state variables. On the other hand, all mathematical dynamical models suffer from neglected physics, inadequate resolution, erroneous forcing data and errors in the initial and boundary conditions. Ghil and Lemusiaux (cited in Brink and Robinson (1998)) state: *"a well constructed melded estimate should agree with all observations within data error bounds and satisfy the dynamical model within model error bounds"*.

The concepts can also be classified with respect to the time interval of the data input for the estimate time (Gelb, 1974). An estimation is said to be a *filtering process* if only past and present data are utilized. A *smoothing process* is a process in which future as well as past and present data are included in the estimate. Brink and Robinson (1998) refer to estimates by either a filtering or a smoothing process as *data-driven simulation*.

The objective of this thesis, drawing from the above discussion, is to implement, test and apply a scheme for combining observations with a regional ocean model that can be applied for multi-decadal simulations. Because of the large computing costs of such simulations and the restricted availability of observational data for long periods, such a scheme should meet the following requirements:

1. It should be simple and cost-efficient
2. It should utilize only observational data
    - which are available on multi-decadal time scales
    - which have sufficient accuracy
    - which are sufficiently homogeneous on multi-decadal time scales
    - which are available at high spatial and temporal detail.

So far, sea level measurements from tide gauges represent one of the best possible choices to meet the second requirement. Satellite data are available

only for periods that are still too short for multi-decadal simulations. In order to meet the first constraint, a simple nudging scheme that requires only marginal extra computing costs was adopted.

The thesis is structured as follows:

- The method to combine observations with the model is in this thesis applied on the North Sea. A short description of the dynamics and the history of development of the North Sea is presented in Chap. 2.
- The methods and data used in the thesis are listed in Chap. 3. First methods to combine observations with models and the chosen nudging scheme are reviewed, second the model and data and finally the methods used to calculate surge and trends are described.
- The results are presented and discussed in Chap. 4. In the first section the model is validated with respect to observations. The second section focuses on the sensitivity and validation of the nudging scheme. In the third section, results from a 44 year hindcast, with observations from the tide gauge Aberdeen nudged are presented. The improvement by nudging is quantified and the extreme sea level heights are given more detailed consideration. In the last section the long-term changes and inter-annual variability of extreme events are investigated and an improved description of long-term changes in the North Sea is presented.
- The thesis is concluded in Chap. 5, and outlooks for the future are presented.

Chapter 2

The North Sea

The North Sea is located on the Northwestern European Continental Shelf and represents a shallow sea with depths mostly up to 200 m. An exception is the Norwegian Trench along the Norwegian coast where depths reach values of up to 700 m (See also the bathymetry used in the model, which is presented in Fig. 3.2 in Sec. 3.2.2). The North Sea extends approximately 400 km in the east-west direction and 800 km from north to south. The southern North Sea is up to 50 meters deep, while the northern part has depths of up to 200 meters.

Tidal waves enter the North Sea basin from the Northwest and from the Southwest through the English Channel (Pugh, 1987). According to Høyer and Andersen (2003) the North Sea mean circulation is cyclonic (Fig. 2.1) with an average transport of about 1 Sv (10^6 $m^3 s^{-1}$) and a mean flushing time of about 650 days. Huthnance (1997) reported annual averages of Atlantic inflow of approximately 1.7 Sv and 0.1 Sv inflow through the Strait of Dover, which both are highly variable and show strong seasonal variations. It takes one to three years for the complete renewal of the water in the North Sea (Sündermann et al., 2002).

Summer warming leads to a vertical stratification of the water masses near the surface, and the influxes of freshwater from the Baltic and the large rivers cause horizontal fronts with strong salinity gradients. The North Sea is one of the most productive marine regions in the world (Sündermann et al., 2002), and the marine ecosystem, from plankton to fish and mammals, have adapted to this baroclinic regime.

Figure 2.1: Water circulation in the North Sea (dark blue) and Atlantic inflow (light blue). The width of the arrows indicates the magnitude of the water transport. (Sündermann et al. (2002), adopted from OSPAR.)

Sea level observations in the North Sea are dominated by tidal signals from the harmonic components M_2, S_2, O_1 and P_1. However, nonlinear shallow water tidal constituents such as M_4 and MS_4 also contribute significantly to the observed water level variations (e.g., Pugh 1987, Høyer and Andersen 2003). The latter is a result of shallow water effects in the advection and bottom friction term in the shallow water momentum equation that are not negligible for small water depths. An overview of other tidal constituents and their frequencies are shown in Tab. 3.2.

Shallow water theory predicts a counter-clockwise propagation of the tide-surges resembling a Kelvin wave (Pugh, 1987) with speed

$$c = \sqrt{gH},$$

where g is gravity and H is the water depth. The offshore scale of the sea surface height variations is given by the barotropic Rossby radius a,

$$a = \frac{c}{f},$$

where f is the Coriolis parameter. According to theory, the amplitude of Kelvin waves is related to the water depth as $H^{-1/2}$. A change in water

depth from 150 m in the Northwest to about 10 m in the German Bight corresponds to an amplitude increase of a factor of four. Apart from tidal variation, storm surges also contribute significantly to the sea level height and its variability in the Southern part of the North Sea. The large variations in sea level height, in the order of meters in the North Sea, are contrary to e.g., the Mediterranean Sea where variations in the order of only centimeters are observed.

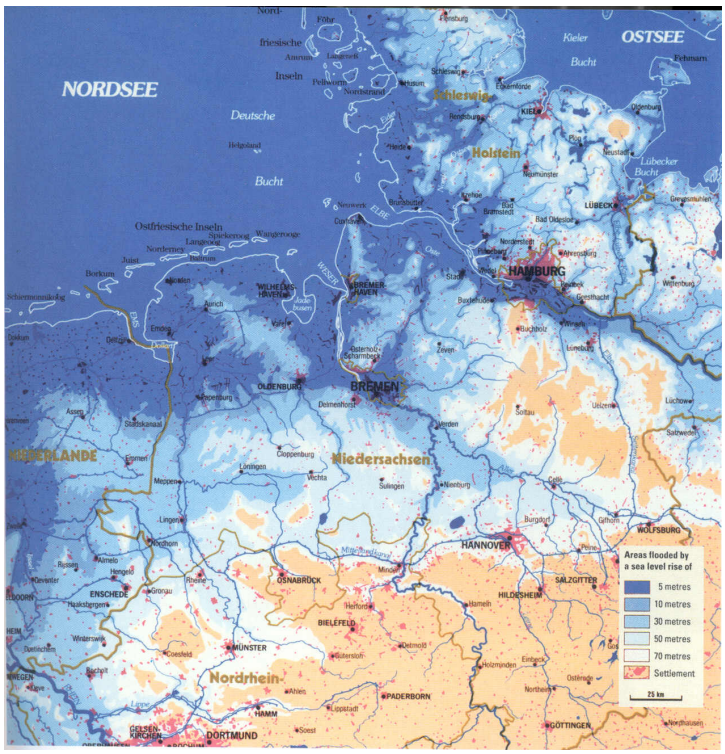

Figure 2.2: Potential flooding of Northwest Europe under rising sea level. A rise of 5 meters would flood considerably large parts of the North German Plain. (Sündermann et al. (2002), adopted from Detlef Maiwald/Studio für Landkarten-Technik, Norderstedt.)

The threat of flooding is important in the areas around the German Bight. Since the last great ice age, approximately 20 000 years ago, sea level has risen worldwide by about 100 meters (Sündermann et al., 2002). During the last 2000 years this rise has ceased. Coastlines became heavily populated, and active coastal defense against storm surges more and more common. Storm surges are transient, extreme sea level increases caused by storms. During a storm surge sea level can increase by several meters and in extreme cases overtop or destroy dikes built to protect people from such episodes. Hence, coastline defense has high national and European priority, and in Germany alone 100 million euro are spent on coastal defense every year.

Meteorological effects may be important for the inflows. Especially in the winter season, low pressure areas in the North Atlantic can increase the inflow of water into the North Sea. This phenomenon is commonly referred to as an external surge (See also Section 3.2.4) as the surge was generated external of the North Sea. Here such effects provide an essential contribution to the overall storm surge variability and in particular to extreme events (e.g., Koopmann 1962). In addition to the rise in sea level height caused by an external surge, the inflow from the North Atlantic is an important contributer to the mixing of the water (Sündermann et al., 2002).

Around 30 million people live in the particularly endangered region of the southern North Sea today (Sündermann et al., 2002). A rise in mean sea level could be disastrous for this area, and Fig. 2.2 illustrates which areas are particularly endangered by floods or a rise in sea level. Additionally, human activities, such as dredging of rivers to allow deep draft ships to reach the ports (e.g., the river Elbe and the German city Hamburg), has destroyed much of the shallow forelands and increased the flood risk. The shallow forelands serve as large natural water retention areas over which high water could be dispersed in the past.

Flooding catastrophes occur frequently in the German Bight. In 1362 hundred thousand lives were purportedly lost on the German North Sea coast during the "Marcellus" flood. The storm surge of 31 January-1 February 1953 was one of the most devastating natural disasters in Western Europe in the last century with the loss of over 1800 lives in the Netherlands and 300 deaths in southeast England (Wolf and Flather, 2005). A more recent episode is the well known flood in February 1962, which destroyed the tidal protection system and flooded large parts of the German city of Hamburg and took more than 300 lives. This episode was an example of the previously described external surge phenomenon (Koopmann, 1962).

Due to the relative shallow German Bight, strong winds over long periods can create strong storm surges, which the coastal protection construction must resist. In a changing climate it is also important to predict what will happen in the future. An important indicator for the North Sea climate is the NAO, defined as the difference in air pressure between the Azores High and Icelandic Low. An high index is associated with particularly strong westerly winds and mild stormy winters in the North Sea. Climate scenarios with an increased CO_2 emmision are predicting a changed storm surge climate with an increased probability of extreme floods. Especially in the Netherlands, Germany and Denmark a significant effort is put into calculating and preventing impacts from storm surges.

Chapter 3

Methods and data

The reasoning and history behind combining observational data with models was explained in the introduction. In this chapter different methods are reviewed and the one selected in this thesis is explained and justified in Sec. 3.1 and compared with the other methods. The regional ocean model used for the experiments is described in Sec. 3.2 together with the data used and the outlining of the experimental strategy is presented. The chapter is concluded with a description on how surge and the significance of trends have been calculated.

3.1 Nudging to combine data with observations

Presently a large variety of techniques to combine observations with a model simulation exist. They are extensively described in the literature, and overviews are given by e.g., Daley (1991), Anderson et al. (1996) and Brink and Robinson (1998). Generally, techniques can be divided in two general concepts, "The variational/adjoint method" (Sec. 3.1.1) and "The sequential method" (Sec. 3.1.2). Below a short description of the two different approaches is given. The method used to combine data with an ocean model in this thesis is a sequential nudging method presented in Sec. 3.1.5. To get an overview over the two approaches and their differences, the variational method is first very briefly described. As a background for why the nudging method is chosen, the Kalman filter and a summary of how observed values are combined with ocean models today is presented. A common notation in terms of data assimilation is to use the term state vector, which is a vector containing all variables to be investigated in the state space, and this notation is adopted in the following sections.

3.1.1 The variational/adjoint method (Control Theory)

The variational/adjoint method has been the scheme most often employed (Evensen, 1993). The appeal of the variational procedures is that they consider the system as a whole and do not deal explicitly with the individual components of the system. All approaches perform a global time/space adjustment of the model solution to the complete set of available observations. Hence it can be considered a smoothing problem. Variational methods, in contrast to sequential methods, have feedback to previous times by minimization of a cost function penalizing the time/space misfit between the data and the model estimate, which is constrained by the dynamics included in the model. Normally one separates between methods with strong or weak constraints.

If the model is assumed to be exact, the method is considered to be a strong constraint and leads to the *adjoint method*. The state variables will evolve according to the dynamics included in the model. The method is deterministic and fixed if initial and boundary conditions are provided. A detailed description of the method can be found in e.g., Brink and Robinson (1998) and Daley (1991).

If the model is considered a weak constraint, the smoothing estimate is only in approximate consistency with the dynamical model equations. This assumption includes the possibility of model errors. However, one can argue, depending on the data, model weights and shape of the cost function, any desired field estimate could be made a solution of the variational problem by manipulating the cost function (Brink and Robinson, 1998). The strong constraint is in fact just one of these manipulations. The variational method is a good choice for parameter estimation due to its variational properties.

All problems in which an unknown estimate is calculated from a known set of consequences are called inverse modeling, and the difference between the *generalized inverse problem* (GIP) and the adjoint method is that the model is allowed to differ from the true value and therefore is considered a weak constraint.

The minimization of the cost function for GIP produces the Euler-Lagrange equations as for an adjoint problem, however, with an extra term in the forward integration because the model is no longer assumed perfect. This extra term combines the adjoint equation and the forward equation for the state vector. This coupling makes the use of the adjoint method difficult for the generalized inverse problem, and as a consequence, four other approaches are frequently used. The first approach (*Representer Method*) is

an "expanded adjoint method" for the generalized inverse methods solving the general Euler-Lagrange equations, which leads to the uncoupled set of equations given in e.g., Brink and Robinson (1998) and Evensen (1994a). However, the calculation of Representer Method is an extremely expensive task, but the method, has according to Evensen (1994a), resulted in improvements from the official meteorological forecasts. The three other approaches (*Decent Methods*, *Simulated Annealing* and *Genetic Algorithms*) are direct minimization methods of the cost function, and a closer description can be found in e.g., Brink and Robinson (1998).

3.1.2 The sequential method (Estimation Theory)

Sequential methods use a probabilistic framework and give estimates of the whole system state sequentially by propagating information only forward in time. Deriving an inverse or an adjoint model as for the variational methods is not necessary and makes adaption for all dynamical models easier (Bertino et al., 2003). The probabilistic framework used in the sequential method is also needed to make an estimation of the uncertainties of the results, in contrast to the variational method. In practice, sequential methods are usually a succession of two steps. First, a forecast step is done with a dynamical model. Second, an analysis step is performed, which is a statistical criterion used to meld the incoming data with the forecast.

For a linear system, the Kalman filter (Kalman, 1960) is the sequential, unbiased, minimum error variance estimate based on a *linear* combination of all past measurements and past *linear* dynamics (Kalman 1960, Brink and Robinson 1998). The error variance of the Kalman filter is less than or equal to that of any other unbiased and linear filtering estimate, and because most other sequential methods can be seen as simplifications or compared with the Kalman filter, the method is briefly outlined here.

If you define a linear operator A between each timestep k, you can formulate a discretisized linear model where $\mathbf{w}$ contains the unbiased model noise accounting for the deviation from the true state. This noise accounts for the errors in the mathematical method and the numerical method of approximation. $\mathbf{v}$ is a vector containing the unbiased measurement noise, such as instrumental noise and accounts for the deviation from the true state for the observed value. Thus one can express the true values, ^{t}, for the evolving state vector and the observations as:

$$\boldsymbol{\psi}_k^t = \mathbf{A}_{k-1}\boldsymbol{\psi}_{k-1}^t + \mathbf{w}_{k-1} \tag{3.1}$$

$$\mathbf{z}_k = \mathbf{H}_k\boldsymbol{\psi}_k^t + \mathbf{v}_k \tag{3.2}$$

The available observations are $\mathbf{z}_k$; $\mathbf{H}_k$ is the measurement matrix linking the measurements to the state vector $\boldsymbol{\psi}$. The classic deterministic version of the Kalman filter is achieved when one assumes that the observation error is uncorrelated with the model error. The forward integration of the state vector and error propagation matrix $\mathbf{P}$ can be expressed as:

$$\boldsymbol{\psi}_k^f = \mathbf{A}_{k-1}\boldsymbol{\psi}_{k-1}^a \tag{3.3}$$

$$\mathbf{P}_k^f = \mathbf{A}_{k-1}\mathbf{P}_{k-1}^a\mathbf{A}_{k-1}^T + \mathbf{Q}_{k-1} \tag{3.4}$$

The optimal melding of the data in a least square sense for the two forecasts above is:

$$\boldsymbol{\psi}_k^a = \boldsymbol{\psi}_k^f + \mathbf{K}_k[\mathbf{z}_k - \mathbf{H}_k\boldsymbol{\psi}_k^f] \tag{3.5}$$

$$\mathbf{K}_k = \mathbf{P}_k^f\mathbf{H}_k^T[\mathbf{H}_k\mathbf{P}_k^f\mathbf{H}_k^T - \mathbf{R_k}]^{-1} \tag{3.6}$$

$$\mathbf{P}_k^a = \mathbf{P}_k^f - \mathbf{K}_k\mathbf{H}_k\mathbf{P}_k^f \tag{3.7}$$

Superscripts ^{f}, ^{a} and ^{T} are forecasted, analyzed/updated values and vector transposed respectively. $\mathbf{Q} = \epsilon[\mathbf{w}_{k-1}\mathbf{w}_{k-1}^T]$ is the system error covariance matrix which is added to the dynamical evolution of the error propagation matrix $\mathbf{P}$. The error covariance matrix of the observational error is defined as $\mathbf{R} = \epsilon[\mathbf{v}_k\mathbf{v}_k^T]$. $\mathbf{K}_k$ is the Kalman gain matrix, which is the optimal combination of observations with the model. After one estimation the error is reduced, and the propagation of the errors (Eq. 3.4) are updated (Eq. 3.7). In this sense one can say that the data assimilation method learns from its earlier errors.

The Kalman filter can be viewed as a simplification of the general Bayesian estimation (Brink and Robinson, 1998). Both Bayesian theory with the maximum entropy principle and the direct minimum error variance with a linear estimate lead to the Kalman Filter algorithm.

A good and simple example of the properties of the Kalman Filter can be found in Evensen (1992), who solved the linear one-dimensional advection equation by applying a Kalman Filter. The assimilation method knows nothing about the solution at the start time but gets information from two of 30 data points. After just a few updates with the available information the filter is able to reproduce a good representation of exact solution.

Several other sequential methods exist. The different sequential methods mainly differ in the way the statistical approach, used as background for the melding step, is done. Mainly they can be considered as simplifications of the Kalman filter and they are comprehensively described in literature, e.g., Brink and Robinson (1998), Daley (1991), Jazwinski (1970) and Gelb (1974). For this reason and because the method used to combine observations with the model simulations later in the thesis is more extensively described in Sec. 3.1.5, the different methods are only summarized in the following paragraphs.

As the name states, *successive corrections* corrects the forecast several times, instead of just giving a linear combination of the data and the forecast. The method is iterated until it reaches a given threshold. The weighting matrix combining the observations with the model is, as for Optimal Interpolation (see under), empirically assigned. Normally only two or three iterations are performed (Daley, 1991), and the matrix should be a function of feasible processes and scales for the actual problem (e.g., geostrophical approximation for a synoptic scale problem). The iteration limit of the method was further investigated by Bratseth (1986) and reformulated so that it conformed with the method of Optimal Interpolation.

Both terms *Optimal interpolation* and *Statistical interpolation* are widely used, but describe the same method. The linear combination is very similar to Eq. 3.5, but the Kalman gain K is substituted by an empirically assigned matrix (gain matrix). Normally this gain matrix is based on empirical forecast error covariance matrix, which will create a consistent description of the error covariance. Contrary to the Kalman filter the gain matrix will not develop internally according to the model system but is empirically assigned. If the gain matrix is held constant over time, it is equivalent to the matrix of nudging coefficients in the nudging method (see under), with the exception that the gain matrix does not need to be diagonal.

Nudging can be seen either as a simplification of the Kalman Filter with an empirically assigned Kalman gain matrix or as the dynamical model relaxed toward the observations. Another nudging approach is the *spectral nudging* applied by Waldron et al. (1996) and von Storch et al. (2000). The theoretical background is the same, but the analysis is performed in the spectral space. Especially for down-scaling purposes this might be a good approach (von Storch et al., 2000). The method applied for this thesis can be seen as an example of nudging and is detailed explained in Sec. 3.1.5.

Blending is a linear combination of the forecasted value and the observed data. The observed data are not assumed to be perfect but are just updated for data points where observations are available.

Direct insertion is the most extreme variant of sequential data assimilation. For all data points with available observations the forecasted value is directly replaced with the observation.

3.1.3 Non-linear problems

The methods described so far are outlined for a linear model. Although the Kalman filter is optimal for a linear model, one has to remember that most dynamical systems such as the ocean and atmosphere have a strongly non-linear behavior. The methods remain but with adjustments for non-linearity. The extended Kalman Filter has an expansion of the development of the error covariance propagation matrix (P in Eq. 3.7) and has been used for non-linear models (e.g., Heemink and Kloosterhuis 1990).

Energy is accumulated at high wave numbers in a non-linear model and Evensen (1992) used a damping method (Shapiro filter) to control the instability. The results in Evensen (1992) were produced with closed boundary conditions, and open boundary problems were discussed in Evensen (1993). Hence, Evensen (1994b) suggested that the unbounded error growth found in the extended Kalman Filter, which is caused by a simplified closure of the error covariance equation, could be eliminated by using an Ensemble Kalman Filter. The filter has basically the same properties as the Extended Kalman filter but uses a Monte Carlo approach to forecast the error covariance propagation. In this matter one does not need any closure of the error covariance equation and the non-linearities treated by the model, but nevertheless additional computations are needed to create an ensemble. Promising results of works performed with Ensemble Kalman filter are e.g., Allen et al. (2000), Haugen and Evensen (2002) and Johannesen et al. (1993).

Another approach of using the Extended Kalman filter are the Reduced Rank Square Root (RRSQRT) and Singular Evolutive Extended Kalman (SEEK) filter. Both methods are sub-optimal as they simplify the error covariance matrix by an eigen-decomposition and approximate the covariance by a low number of dominant eigenmodes. The RRSQRT method suggested by Heemink et al. (1997) reduces the rank of the error covariance matrix based on the eigen-decomposition and uses the values of the highest eigenvalues. The SEEK filter discussed in Brasseur et al. (1999) is based on singular forecast and analysis error covariance matrices. Bertino et al. (2003) discuss both methods further and point out that the main weakness is the error analysis depending on the initial error and the schemes suboptimal nature.

3.1.4 Combining observations with an ocean model

Many of the previously explained techniques of combining observations with models have originally been developed and applied in atmospheric sciences. For ocean modeling, data assimilation represents a relatively new research area. According to Brink and Robinson (1998), earliest attempts date back to 1982, when Bennett and McIntosh (1982) used a weighted variational approach to include reliable sea level data from the coastline in addition to ad-hoc open boundary conditions. More recently, most of the more sophisticated techniques mentioned above have been applied to oceanography, however, only for relatively short periods of time. In this section some of the ongoing projects in ocean research utilizing some form of data assimilation are described.

On a global scale the project ECCO[1] uses a global ocean model and its adjoint (Sec. 3.1.1) constrained by TOPEX/POSEIDON altimeter data. The goal of this project is to obtain the best possible estimate of the time evolving ocean circulation and related uncertainties. The MERSEA[2] integrated project is developing a European system for operational monitoring and forecasting of the ocean physics, biogeochemistry, and ecosystems with data assimilation included on global and regional scales. The system to be developed will be a key component of the Ocean and Marine services element of GMES[3]. Danmarks Meteorologiske Institut (DMI) as a part of the MERSEA project presently produces forecasts every 12 hours of physical parameters for the North Sea-Baltic Sea system with a regional ocean model. The resolution of the model is 6 nm with a small nested domain of 1 nm resolution in the southern part of the Danish waters (Fehmarn Belt) and the forecasting length is at present 54 hours. Data assimilation of sea surface temperature and sea level height and ecological modeling is or will be introduced into the operational setup.

Presently, sea level represents the most common variable used for data assimilation in regional ocean models (e.g., Zhang et al. 2002, Haugen and Evensen 2002), first because it is a major variable for tide-surge modeling as the barotropic circulation is completely determined by spatial sea level gradients, second because it represents so far one of the best and most frequently observed ocean quantities from both tide gauges and satellites. More re-

[1] Estimating the Circulation and Climate of the Ocean
`http://www.ecco-group.org/`

[2] Marine Environment and Security for the European Area
`http://www.mersea.eu.org/`

[3] Global Monitoring for Environment and Security
`http://www.gmes.info/`

cently, efforts have been made to also assimilate other variables such as temperature (e.g., Keppenne and Rienecker 2003, Haugen and Evensen 2002) or phytoplankton for eco-system modeling (e.g., Johannesen et al. 1993, Allen et al. 2000). The ongoing project CCDAS[4] is working on setting up a carbon cycle data assimilation system to improve the modeling of the carbon cycle by exploiting existing data sources (e.g., flux measurements, carbon inventory data, satellite products).

3.1.5 Nudging scheme

So far, all data assimilation efforts in ocean modeling have focused on the simulation of relatively short periods, up to a couple of years, concentrating mainly on the improvements that can be obtained from data assimilation (e.g., Høyer and Andersen 2003) or on their applicability for routine forecasts (e.g., Cañizares et al. 2001). Because of the extensive computer resources required by more sophisticated data assimilation schemes, Aspelien and Weisse (2005) reported that to their knowledge no multi-decadal simulation utilizing any form of data assimilation has been performed so far.

The objective of this PhD thesis is to implement, test and apply a method to combine observations with data which is applicable to multi-decadal ocean simulations. Such a method should meet the following requirements:

1. It should be simple and cost-efficient, a requirement that is hardly fulfilled by most of the schemes discussed above.
2. It should utilize only observational data
    - which are available on multi-decadal time scales
    - which have sufficient accuracy
    - which are sufficiently homogeneous on multi-decadal time scales
    - which are available at high spatial and temporal detail.

In order to meet the first constraint, a simple nudging scheme, which requires only marginal extra computing costs, was adopted. So far, sea level measurements from tide gauges represent one of the best possible choices to meet the second requirement. Satellite data are available only for periods that are still too short for multi-decadal simulations. Due to the rapid

[4] Carbon Cycle Data Assimilation System
`http://www.ccdas.org/`

development of computational power more advanced methods are normally used to combine observations with models. The field of data assimilation is among many thought of combining observations with models by more advanced methods like the Kalman filter, and for this reason the terminology data-driven modeling, used by e.g., Brink and Robinson (1998), is adopted in this PhD thesis, in which the simpler and more cost-efficient nudging scheme is used. When the method is used to combine observations from a tide gauge with the model, the notation "tide gauge is nudged" is used.

Generally, nudging refers to a relaxation of the model towards a measured value. The relaxation may be combined with a linear interpolation using a weighting matrix based on an empirical weighting function. The method can be compared to Eqs. 3.3-3.7 for the Kalman filter. If the state vector $\boldsymbol{\psi}$ is replaced by e as only the observed sea surface height e is combined with the model, the relaxation (analog to Eq. 3.5) can be expressed by

$$e^a = e^f + W(e^o - e^f) \tag{3.8}$$

where the superscripts a, f and o refer to the analysis, the forecast, and the observation respectively. W represents an empirical weighting function defined by

$$W = \alpha \; exp(-\frac{r^2}{2L^2}). \tag{3.9}$$

The Kalman gain $\mathbf{K}$ is reduced to the empirical weighting function W as only one state variable e is combined with the model. Here r measures the distance between the model grid point and the location of the observations while L refers to a characteristic length scale within which observations will have a significant influence on the analyzed value e^a. The quality of the observations is taken into account by the empirical nudging coefficient α with $\alpha = 1$ indicating perfect observations. An example of a weight function with $L = 60$ km and $L = 30$ km is shown in Fig. 3.1.

From the filtering point of view, the nudging scheme is a simplification of the Kalman filter, where the Kalman gain (Eq. 3.6) is assigned and diagonal (Eq. 3.3 and Eq. 3.5 with $\mathbf{R}_k$, $\mathbf{Q}_k$ and $\mathbf{P}_k^a$ diagonal) (Brink and Robinson, 1998). As in the scheme outlined here the simplified diagonal gain is normally chosen to be constant, but in principle it could vary with time.

Eqs. (3.8) and (3.9) can formally be applied to all model grid points $i = 1, 2, \ldots, M$. When several measurements are available within the prescribed influence area for a particular time, weights are computed taking these N observations into account by

$$e_i^a = e_i^f + \sum_{n=1}^{N} \frac{W_{in}}{\sum_{j=1}^{N} W_{ij}} W_{in}(e_n^o - e_i^f). \tag{3.10}$$

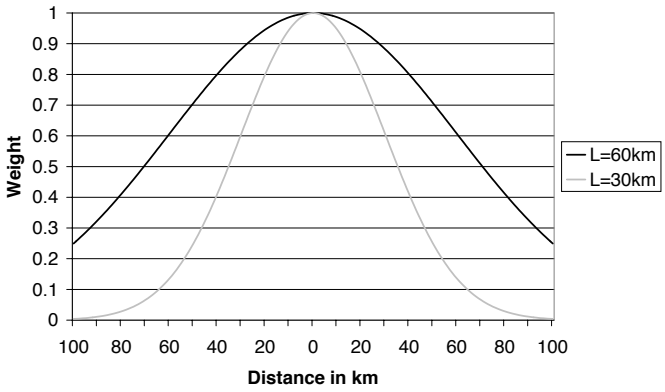

Figure 3.1: Examples of weight function (Eq. 3.9) dependent on distance from observation point with decorrelation radius $L = 60$ km (black) and $L = 30$ km (grey). α is in both cases 1.0

Although this nudging scheme is rather simple, it has several advantages with respect to multi-decadal simulations: It is cheap in terms of the additional computing power required, and (as weights are determined independently for each model grid point and time step) data gaps and/or varying locations of the measurements can easily be taken into account.

3.2 Model and data

In this study a regional ocean model is used. The model, together with the experimental setup and strategy is briefly described in this section. Additionally, the data and some of the specific methods used in this thesis are explained. The model is validated against observations from coastal tide gauges and the results are compared with literature in Sec. 4.1.

3.2.1 TRIMGEO

The regional ocean model TRIMGEO (Tidal Residual and Intertidal Mudflat model with geographical coordinates) was set up for the North Sea. The model operates on an Arakawa C-grid (Mesinger and Arakawa, 1976) and is

based on the primitive equations. More information about the model can be found in Casulli and Cattani (1994) and Casulli and Stelling (1998). The model TRIMGEO has also been used for downscaling of climate scenarios (Woth et al., 2005) with satisfactory results for the North Sea.

Generally, the equations in TRIMGEO are solved on a three-dimensional grid. In this thesis, a depth averaged two-dimensional version was adopted. This choice was motivated by the fact that model experiments for the North Sea showed only minor differences between two and three-dimensional simulations when sea level was analyzed (Kauker and Langenberg, 2000). As only tide gauge data are available for multi-decadal assimilation experiments and as sea level and surge is to be investigated in this thesis, the choice of the two dimensional version appears to be justified. The bottom friction in the model is parameterized by Manning coefficients (Soulsby, 1997), and the friction is dependent on current velocity (Taylor parameterization). In addition, the depth of the bottom layer is taken into account (exponential velocity profile).

3.2.2 Model setup and data

The model was integrated at a spatial resolution of $\frac{1}{6} \times \frac{1}{10}$ degree in zonal and meridional direction respectively. The model domain extends from 4.25° West to 13.42° East and from 48.55° to 59.75° North. A time step of 10 minutes was adopted. The bathymetry (Fig. 3.2) was provided by the German Federal Maritime and Hydrographic Agency (BSH) and is identical with that used in their operational system. The model was run with open boundaries at 59.75 N and in the English Channel, while in the eastern part of the model domain closed boundary conditions were adopted. Fresh water inflow from the Baltic Sea was parameterized as 0.01498 $m^3 s^{-1}$ (OSPAR Commision, 2000) and the input of the 33 largest rivers was taken into account using climatological values obtained from the operational forecast system at the BSH (Esselborn, pers. comm. 2003).

In all experiments the model was driven by identical sea level pressure and near-surface wind fields obtained from a regional multi-decadal atmospheric reconstruction (Feser et al., 2001) driven by the National Centers for Environmental Prediction (NCEP) re-analysis (Kalnay et al., 1996). In this regional atmospheric reconstruction special emphasis was given to the quality of near-surface marine wind fields (Weisse et al., 2003), and Weisse and Feser (2003) have shown that the modeled wind fields compare well with in-situ measurements. Because the spatial resolution of the atmospheric data is about 50 $km \times 50$ km they have been interpolated bi-linearly to TRIMGEO resolution for this study.

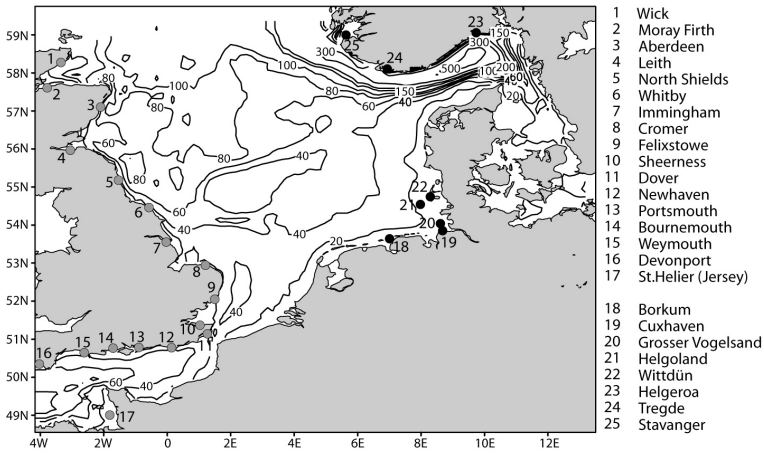

Figure 3.2: Bathymetry and location of the tide gauges used for nudging (1-17 in grey) and validation (18-25 in black). Contour lines are drawn for 20, 40, 60, 80,100, 150, 300 and 500 meters depth.

The model is run with open boundaries at 59.75 N and in the English Channel and has the same setup as the operational model at BSH had when TRIMGEO was set up. At the open boundaries, sea level was prescribed from the amplitudes and phases of 17 major tidal constituents. The amplitude and phase are given for each boundary point and are calculated from previously used moorings at the northern boundary. For the open boundary points in the English Channel, published harmonic components (e.g., d'Hieres and Provost 1978) were adopted (Dick & Esselborn, pers. comm).

The tide gauges with data used in this thesis are shown in Fig. 3.2. The tide gauge data for United Kingdom (UK) (gauge 1-17 in Fig. 3.2) were provided from the British Oceanographic Data Centre (BODC). Some of the data were hourly sampled and some at a 15 minute interval, and values were relative to chart datum (CD). The heights of chart datum relative to ordnance datum (OD) for the English tide gauges were not known at the beginning of the work, and for simplicity the yearly mean value of the observed heights is assumed to correspond with the model's zero level.

The German tide gauges are numbered from 18-22 in Fig. 3.2. ODs for the German Tide gauges were provided from BSH, which also provided parts of the German tide gauge data. These data were mostly hourly sampled. German Federal Waterways Engineering and Research Institute (BAW) provided the other German data of high and low waters.

The Norwegian tide gauge data (gauge 23-25 in Fig. 3.2) were given relative to Norwegian zero level, and the values were used directly for comparison with model results. The data used for this work were provided from Statens Kartverk (sjø) and had a 10 minute sampling interval.

3.2.3 Experimental setup

For our analysis the available tide gauge data were divided into a nudging and a validation data set. The data set for nudging is comprised of data from the 17 British tide gauges while the validation set consists of data from the German and Norwegian tide gauges (Fig. 3.2). This separation was motivated mainly by the prevailing counter-clockwise large-sale circulation and the tidal regime of the North Sea (e.g., Høyer and Andersen 2003, Sündermann et al. 2002) and was performed so that upstream/downstream tide gauges have been used for nudging/validation respectively. First a control simulation (CTL) was performed, where no nudging was applied but which was forced with the same meteorological forcing as the nudged experiments.

Promising results from Weisse and Plüß (2005) motivated the choice of combining observations from Aberdeen with the model. In this thesis observations from Aberdeen are nudged (ABE) and tested in a systematical way together with other approaches. To test if nudging of one of the other UK tide gauges could perform similar results as for Aberdeen, experiments with observations from Whitby (WHI) and Cromer (CRO) were set up. All three tide gauges are located on the eastern UK coast (tide gauges 3,6 and 8 in Fig. 3.2), and the experiments are listed in the upper Tab. 3.1. The UK coastline has a relatively simple bathymetry, and for simplicity the observations from the tide gauges were trusted and the nudging coefficient α set to 1.0.

Nudging of a single tide gauge is very cost-efficient in the model setup of TRIMGEO, but to test the improvement by nudging a combination of several tide gauges and different parameters in Eq. 3.9, 6 slightly more computationally demanding experiments were set up (lower Tab. 3.1). They all consist of the 17 British tide gauges (tide gauges 1-17 in Fig. 3.2). As some of the tide gauges are located in close geographical proximity, one interesting test is to investigate the sensitivity of the method to varying influence of the observations. Three different experiments with decorrelation radius of 60 km were set up, in which the nudging coefficient α was varied among $\alpha = 0.5$ (N65), $\alpha = 0.9$ (N69) and $\alpha = 1.0$ (N6U).

The horizontal decorrelation scale of storm surges is generally much larger than that of non-tidal currents or the velocities of advected, buoyant objects such as oil slicks or life-rafts (UNESCO, 2003). Spatial differences in sea level are related to horizontal integrals of surface currents and wind stress and therefore tend to be of larger scale than current and wind. For this reason the sensitivity of the method due to a different decorrelation radius ($L = 30$ km) was tested for the fully nudged experiments. The nudging coefficient α was varied between $\alpha = 0.5$ (N35), $\alpha = 0.9$ (N39) and $\alpha = 1.0$ (N3U). The decorrelation radii as a function of spatial distance from an observation are illustrated in Fig. 3.1 for $L = 60$ km and $L = 30$ km. The experiments in which all UK tide gauges are nudged are named after the decorrelation radius and the nudging coefficient used, the first letter N meaning all UK tide gauges are nudged, the second number being 3 or 6 indicating a decorrelation radius of 30 or 60 km and the last number being 5,9 or the letter U (unity) which are indicating $\alpha = 0.5$, $\alpha = 0.9$ and $\alpha = 1.0$ (see Tab 3.1).

The area of influence is the horizontal distance from the point of observation for which nudging will be performed. Because the influence of this distance can be manipulated by choosing different decorrelation radii in Eq. 3.9 and because when two or more tide gauges are inside each others area of influence they are linearly interpolated by Eq. 3.10, the area of influence in all experiments was chosen to 100 km.

Nudged experiments			
Single tide gauge nudged			
	$\alpha = 1.0$	$\alpha = 1.0$	$\alpha = 1.0$
$L = 60$ km	ABE	WHI	CRO
All UK tide gauges nudged			
	$\alpha = 0.5$	$\alpha = 0.9$	$\alpha = 1.0$
$L = 60$ km	N65	N69	N6U
$L = 30$ km	N35	N39	N3U

Table 3.1: Upper Tab.: Experiments and nudging parameters where single tide gauges are nudged. Lower Tab.: Experiments and nudging parameters where 17 tide gauges at the UK East coast line and in the English channel are nudged.

3.2.4 Calculation of surge

The meteorological part of the sea level height which is not influenced by external astronomical (celestial) forces is normally called surge (or storm surge). The most important astronomical forcing in the North Sea is the

lunar semi-diurnal tide, M2 (Pugh, 1987). The solar semi-diurnal tide S2 and other partial tide components are also of importance (Høyer and Andersen, 2003).

The perturbation in sea level during a storm is the result of two effects. First, the storm winds exert a stress on the water surface leading to a forced response and to free shallow-water waves that can propagate away from the region of direct forcing to influence the water surface at remote locations. Second, the fall in barometric pressure associated with a storm perturbs the surface. This has often been called the inverse barometer effect.

Water level records in coastal waterways indicate that the the most obvious clue confirming the presence of the tide is a sinusoidal oscillation containing either two main cycles per day (semi-diurnal tides), one cycle per day (diurnal tides), or a combination of the two (mixed tides). The underlying principle of harmonic analysis for tides is that, no matter how complex they may appear, tidal oscillations can be broken down into a collection of simple sinusoids. Each "cosine" wave will have the same period of oscillation as the celestial forcing that gives rise to it.

This idea is based on the fact that all over the world the same frequencies ϕ are governing the tide, however, one has to find the combination for the actual geographical location. This can be expressed as a Fourier-series:

$$h(t) = h_0 + \sum_{k=1}^{N} a_k cos(\omega_k t) + b_k sin(\omega_k t) \tag{3.11}$$

In Eq. 3.11 $h(t)$ is the sea level height at the geographical location calculated for time t. The mean value for the location is h_0 and $\omega = 2\pi\phi t/360$. The N partial tides are the necessary number of partial tides needed to describe the tides. The harmonic constants a_k and b_k can be calculated from the timeseries h with length T by this formula:

$$a(k) = \sum_{t=1}^{T} \frac{h_t cos(\omega_k t)}{cos^2(\omega_k t)} \tag{3.12}$$

$$b(k) = \sum_{t=1}^{T} \frac{h_t sin(\omega_k t)}{sin^2(\omega_k t)} \tag{3.13}$$

In this work a harmonic analysis is performed on observed or modeled sea level height with frequencies ϕ from $N = 30$ partial tides (Tab. 3.2). The mean is first subtracted from the timeseries h, and the timeseries is detrended. Then the harmonical analysis in Eq. 3.11 is performed on the timeseries h. The difference between the water level in timeseries h for

Partial tides and frequencies [deg/hour]			
tide	freq. (ϕ)	tide	freq. (ϕ)
M2	28.9841042	Q1	13.3986609
S2	30.0000000	NUE2	28.5125832
N2	28.4397295	2SM2	31.0158958
K2	30.0821373	S4	60.0000000
MU2	27.9682085	M6	86.9523127
K1	15.0410686	2MS6	87.9682085
O1	13.9430356	MP1	M2 - P1
P1	14.9589314	SO1	S2 - O1
M4	57.9682085	MNS2	M2 + N2 - S2
MS4	58.9841042	MSN2	M2 + S2 - N2
SA	0.04106668	MO3	M2 + O1
SSA	0.08213728	MK3	M2 + K1
MM	0.54437471	MN4	M2 + N2
MF	1.09803304	MK4	M2 + K2
MSF	1.01589576	M8	4 * M2

Table 3.2: Partial tides and frequencies [deg/hour] used to calculate surge in this work.

time t and the water level calculated from Eq. 3.11 for time t is called surge. The resulting surge is smoothed with respect to the two closest time steps backwards and forwards in time. Comparisons of surge calculated from observed and modeled data for the German Bight have shown that the method for calculating surge is appropriate (Weisse, pers comm 2004).

3.2.5 Calculation of significance of trends

Linear trends are calculated in Sec. 4.4. The tested null hypothesis (H_0) is that no trend exists, and a two-sided test is therefore performed with a confidence level of 95%. Different methods exist to calculate the significance of a test. An important criterion is the sample length, and a parametric t-statistics and a non-parametric Mann-Kendall test were tested in this thesis.

It was demonstrated by von Storch (1995) that the existence of positive serial correlation within a timeseries increases the possibility that the Mann-Kendall test detects the significance of a trend. This may lead to rejection of the null hypothesis of no trend while the null hypothesis is actually true. In order to eliminate the influence of serial correlation on the Mann-Kendall test, Kulkarni and von Storch (1995) and von Storch (1995) proposed to pre-

whiten a series prior to applying the Mann-Kendall test. That is the serial correlation is removed by subtraction of an AR(1) process from a timeseries, and the significance of a trend is then evaluated by using the Mann-Kendall test to the pre-whitened series. Yue et al. (2003) argued that if a trend exists it is not certain whether or not pre-whitening can effectively eliminate the effect of serial correlation on the Mann-Kendall test.

Chapter 4

Results

The nudging scheme presented in Sec. 3.1.5 was tested and used in a multi-decadal hindcast. The results are presented as follows: validation of the model (Sec. 4.1), sensitivity of the results by varying parameters of the nudging scheme (Sec. 4.2), results from a hindcast with and without nudging focusing on extreme values (Sec. 4.3), effect of nudging on variability and long-term changes of extreme events (Sec. 4.4). Results for both sea level height (SLH) and surge are shown.

4.1 Model validation

Recently the model TRIMGEO has also been used for downscaling of climate change scenarios (Woth et al., 2005) with satisfactory results for the North Sea for their hindcast simulation. To test if the model is valid for its purpose in the present setup, a 23 month period from January 2000 until December 2001 was chosen. The motivation for this period was the availability of observations for model comparison and the reduced time to perform a model run compared to a longer hindcast.

A control simulation (CTL) was performed in which the model was driven by wind and atmospheric pressure only (Sec. 3.2.3). This simulation is validated with observations. The first task is to determine to what extent the CTL simulation is capable of reproducing observed sea level fluctuations. Figure 4.1 shows the root-mean-square error (RMS) (e.g., von Storch and Zwiers 1999) between modeled and observed sea level height for the CTL simulation together with the standard deviation for the observations from

a number of tide gauges along a section from Wick in the Northwest of the model domain to Stavanger in the Northeast (Fig. 3.2). The section is motivated by the counter-clockwise circulation which is normally observed in the North Sea (Sec. 2).

For the 16 British tide gauges analyzed, the RMS ranges between about 20 and 60 cm with increasing values from North to South. An exception found for Sheerness, for which a RMS of nearly 80 cm was found, perhaps the result of a relatively coarse spatial resolution in the simulations. Apart from Sheerness, largest RMSs were found for two German tide gauges, namely Cuxhaven and Großer Vogelsand, both located in the German Bight.

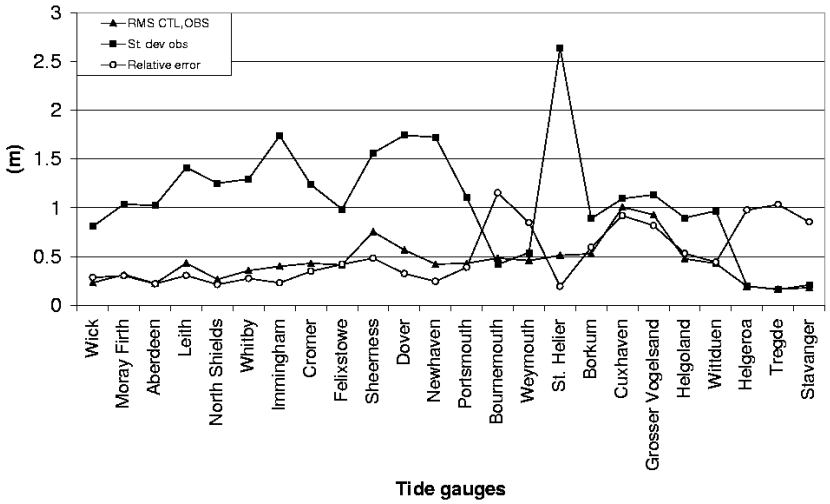

Figure 4.1: Standard deviation of the observed sea surface heights in meters and Root-mean-square-error (RMS) between observed and modeled sea surface heights in the control simulation. The analysis was made with available hourly data for the period 01 January 2000 until 30 November 2001.

The observed standard deviation in Fig 4.1 indicates large variations in observed sea level heights. Standard deviation is the square root of the variance and can be interpreted as a measure of the natural variability. Storm surges provide a particular large contribution to the overall observed sea level variability in the North Sea and the German Bight in particular. This matter will be investigated in more detail in Sec. 4.2 when the sensitivity of the results for the North Sea for different nudging approaches is investigated with

respect to storm surge. At the Norwegian tide gauges, where both storm surges and tidal elevations are smallest, smallest RMSs were obtained.

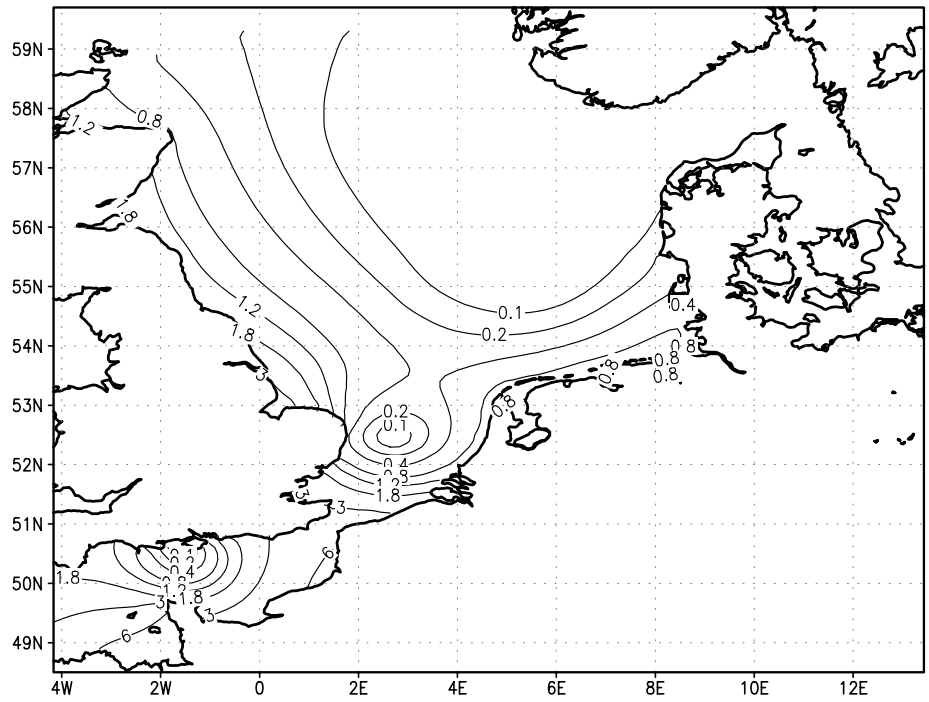

Figure 4.2: Variance of sea level height in m^2 obtained for the control experiment. The analysis used data every 30 minutes from the period 01 January 2000 until 30 November 2001. Contour lines are drawn for 0.1, 0.2, 0.4, 0.8, 1.2, 1.8, 3.0 and 6.0 m^2.

The relative error in Fig. 4.1 (RMS between sea level height from CTL and observed sea level height divided by the observed standard deviation) is smallest for the UK tide gauges with an exception for the tide gauges Portsmouth, Bournemouth and Weymouth located in the English Channel. The Norwegian tide gauges have a large relative error but also a small standard deviation in sea level height. The two tide gauges with the largest RMS, Cuxhaven and Großer Vogelsand, have standard deviation of observed sea level height of almost the same magnitude and a large relative error.

RMS between modeled and observed sea level height is a good measure of the error made of the model in reproducing the observed sea level heights. The model TRIMGEO is used to calculate sea level heights and surge from the modeled sea level height in this thesis. Hence it can be concluded from Fig. 4.1 that the model has a reasonably low RMS outside the English Channel and is valid for its designated purpose.

Generally, sea level variance in the CTL experiment is largest in the coastal zones with largest values obtained for parts of the English Channel (Fig. 4.2). Smallest values were found at about 52.5 N, 2.5 E within the English Channel and off the Norwegian coast. When areas with small sea level variability are interpreted as locations of amphidromic points, Figure 4.2 indicates that the observed large scale variations are reasonably reproduced in the CTL experiment (e.g., Pugh 1987).

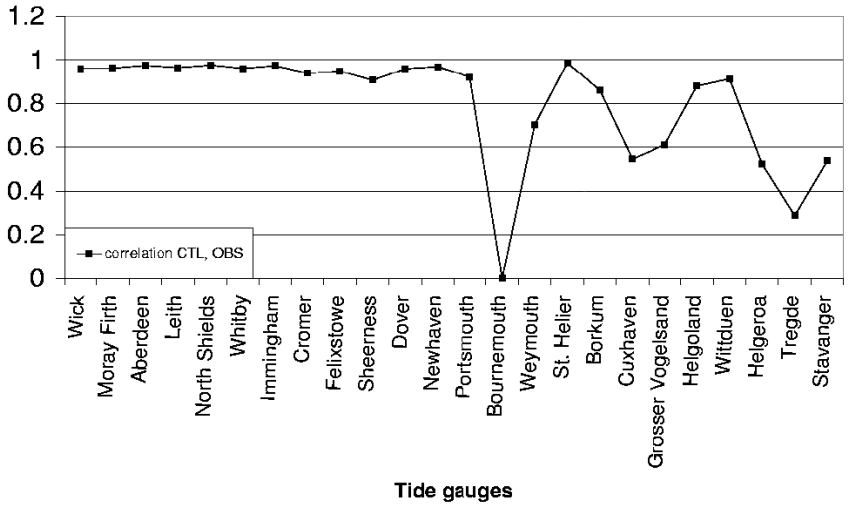

Figure 4.3: Correlation between observed and modeled sea level heights in the control experiment. The analysis was made with available hourly data for the period 01 January 2000 until 30 November 2001.

To investigate the extent to which the observed *phase*, that is, the timing of the maxima and minima of the tide-surge, is reproduced in the CTL experiment, the correlation between observed and modeled sea level height was computed (Figure 4.3). For the British tide gauges, generally, a rather good timing of the tide-surge signal can be inferred. Exceptions are provided by several tide gauges located in the English Channel where the model fails to reproduce phases adequately. The correlation systematically decreases for the German and the Norwegian tide gauges, being lower for the latter. With exception of the tide gauges in the English Channel, the tide gauges with lowest correlation are also the ones with largest relative error in Fig. 4.1.

Summarized one can infer that the model TRIMGEO is valid for the use of modeling sea level heights in the North Sea. The model has difficulties modeling tide gauges in the English Channel but this thesis will not focus on this particular area. TRIMGEO, in Sec. 4.3 and Sec. 4.4, is used to investigate percentiles and long-term trends. For this purpose the model is compared to the observed percentiles and long-term trends in the respective sections.

4.2 Sensitivity of the results to nudging approaches

In section 4.1 the regional ocean model TRIMGEO was tested for its abilities to reproduce observed sea level heights. By introducing a nudging method to combine observations with the model an improved description of sea level variation in the North Sea is expected. By nudging observed data into the model one will not only see effects in close proximity to where model points are adjusted towards observed values but effects will also be seen further away. Dependent on the model dynamics, the new information is transported to other areas.

In this section, the sensitivity of the results for the North Sea due to different parameters in the nudging approach will be investigated in more detail for the time period January 2000 to December 2001. This time span is the same as that used for the validation of the model and is kept to limit computation time for the different experiments. In the following only the tide gauges at the North Sea coast are shown: they are the located in the area of interest and the deviation from the observed sea level height was relatively small (Sec. 3.1). For most of the coastal areas the surge part of the sea level height plays an important role for the local water level for the design and construction of coastal protection measures. The focus in this section is, therefore, set on the surge part of the observed and modeled sea level height.

4.2.1 Variability

In Fig. 4.4 standard deviations of surge for the selected North Sea tide gauges are plotted. For most of the tide gauges at the East coast of Scotland and England the standard deviation of the observed surge is in order of 20 cm, increasing to more than 30 cm for tide gauges in the German Bight. For the selected Norwegian tide gauges a standard deviation of 10 cm for surge is observed. From Fig. 4.4, and the observed standard deviation in Fig 4.1, one can conclude that the surge is an important part of the observed water level in the German Bight. Many of the UK tide gauges have larger variability in the observed water level than the German tide gauges. This indicates that the variability in sea level height for these UK tide gauges is, to a larger extent, controlled by tidal variations.

The CTL experiment was driven with meteorological forcings and Fig. 4.5 shows the ratio of modeled surge from the different experiments in Sec. 3.2.3 and the observed surge from the tide gauges in Fig 4.4. From the curve labeled CTL in Fig. 4.5 it can be stated that storm surge variability is sys-

tematically underestimated by up to 50% in the control experiment. The underestimation is largest close to the northern boundary. This is probably caused by a combination of boundary effects and external processes not accounted for in the present setup of the model and natural variability and extreme events may therefore be underestimated. Boundary effects may comprise artificially limited fetches near the open boundary and may be particularly important in the vicinity of the boundary. Unaccounted external processes involve, for instance, so-called external surges (Sec. 2). They may be particularly relevant for the southern North Sea coast and the shallow German Bight which are located in the inner model domain. The water depth is an important factor for the height of storm surges, and storm surges are larger in shallow areas as the German Bight. Additionally, in the inner parts of the model area, in which the results are better, the wind and sea level pressure included in the model have a longer fetch time.

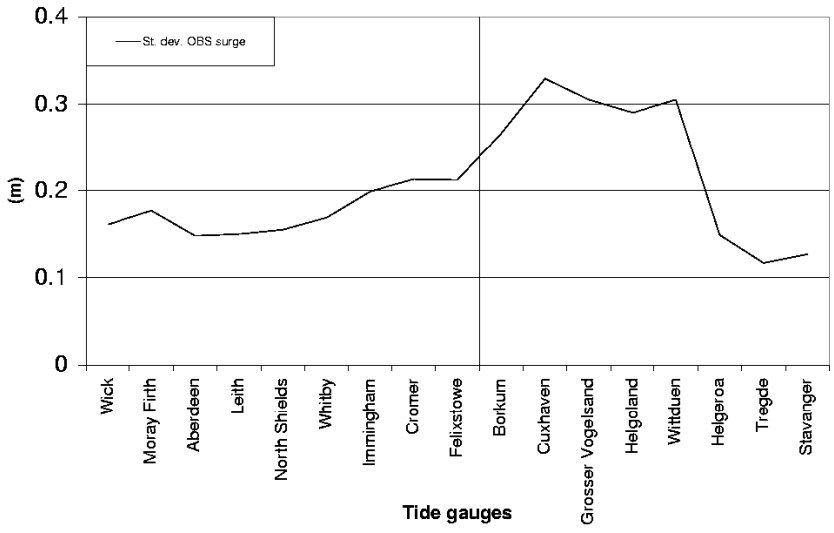

Figure 4.4: Standard deviations of observed surge for the selected North Sea tide gauges. The vertical line is the separation between UK tide gauges at the North Sea coastline which are used in the nudging experiments, and the German and Norwegian tide gauges used to analyze the effect of nudging.

Changes in the representation of modeled surge when different parameters of the nudging scheme are used or additional data are nudged with the model simulation are elaborated first. Fig. 4.5 shows the ratio of standard deviations of modeled and observed surge for different nudging experiments

in comparison with the standard deviation of the CTL experiment. Generally the experiments improve the modeled variability for most of the tide gauges. Especially for the German tide gauges, a large improvement is achieved. One should note that when a single tide gauge is nudged, the surge variability is improved downstream of the nudged tide gauge. Due to the prevailing counter-clockwise circulation and the propagation of the tidal signal in the form of a Kelvin wave, it is not expected that nudging a single tide gauge should improve the variability upstream of the nudged tide gauge.

Generally the different experiments have a relatively similar ratio of the modeled surge for the German and Norwegian tide gauges. For this reason all experiments in Fig. 4.5 are plotted in the same figure so as to illustrate the similar shapes of the curves. The surge calculated from most of the nudged experiments are closer to the observed surge than the CTL experiment, however, the model has difficulties to model the variation of surge at the UK tide gauge Felixstowe and the German tide gauge Borkum, where the standard deviation of modeled surge is greater than the one from observed surge. This is possibly a result of the resolution used in the model setup, consequently Borkum will be investigated in greater detail in Sec 4.4.

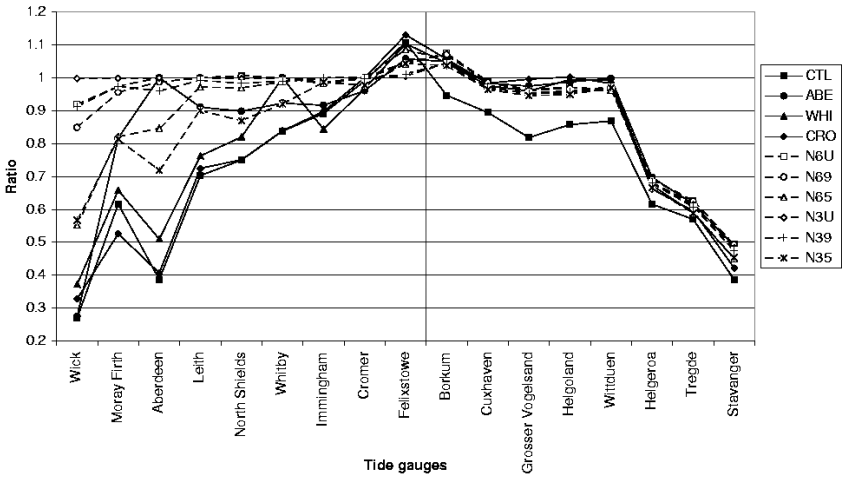

Figure 4.5: Ratio of standard deviations of the surge in the different experiments and the observed standard deviation of surge.

4.2.2 Improvement in surge from nudging

The variability in surge increased towards the observed surge variability when nudging was applied (Fig. 4.5), but does it also approximate the observed surge values? To address this question the effect of nudging one tide gauge is investigated followed by the sensitivity of the results, depending on which tide gauge is nudged. For this purpose the three tide gauges Aberdeen, Whitby and Cromer are chosen (Sec. 3.1). The tide gauges are all located on the eastern UK coastline and are well spatially separated.

Fig. 4.6 shows the ratio of RMS and the standard deviation of observed surge. The RMS is calculated between surge from observations and experiments for which only a single tide gauge is nudged (ABE, WHI and CRO). The RMS was normalized with the standard deviation from the observed surge to get an overview over the relative error. The ratio for ABE and WHI is quite similar downstream of the nudged tide gauge and considerably better than for the control run (CTL). The tide gauges where nudging has been performed are easily identified in Fig. 4.6 with a relative error of zero, as should be expected due to the nudging coefficient $\alpha = 1.0$.

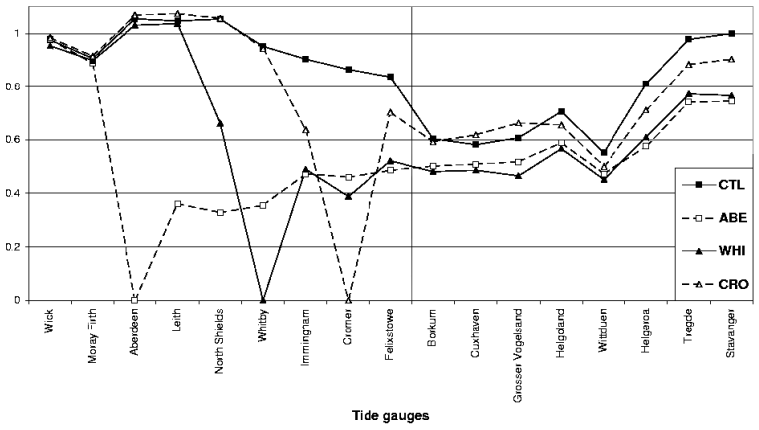

Figure 4.6: Ratio of RMS and the standard deviation of the observed surge (Figure 4.4) for the North Sea tide gauges. The RMS is calculated between surge from the nudged experiments, in which one tide gauge is nudged, and from observed surge.

The CRO experiment does not perform as well as the ABE and WHI experiments and, for several tide gauges is worse than the CTL experiment. From figures of the stream-patterns from the model (not shown) and the North Sea circulation in Fig. 2.1, the speculation can be made that most of the water volumes transported along the coast of East UK to the German Bight do not reach Cromer, where the observations are fed into the model. Cromer is located close to an amphidromic point (Fig. 3.2 and Fig. 4.2) and the local sea level height is influenced more from water masses coming from the English Channel than the tide gauges Whitby and Aberdeen. However, as the ABE experiment improves the surge and reduces the relative error by about 50% at Cromer this explanation seems unlikely. Additionally, there is a high correlation in Fig. 4.3 and the relative error for Cromer in Fig. 4.6 is on the order of magnitude with the rest of the UK tide gauges, indicating that the model is reproducing the sea level height for Cromer reasonably well. No plausible explanation is therefore found for the poorer results by nudging Cromer.

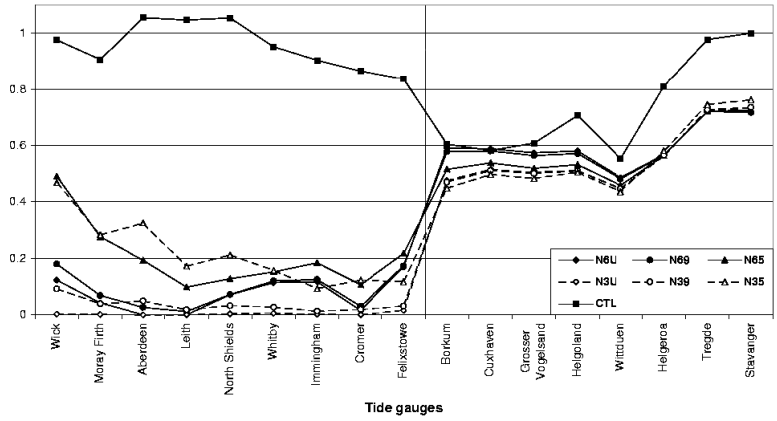

Figure 4.7: Ratio of RMS and the standard deviation of the observed surge (Figure 4.4) for the North Sea tide gauges. The RMS is calculated between surge from the fully nudged experiments and from observed surge.

In the above the sensitivity of the results to the choice of single tide gauges on the East coast of UK to nudge was tested. Following, is a detailed assessment of the sensitivity of the results by nudging the available observations from all the UK tide gauges. Fig. 4.7 shows the ratio of RMS and standard deviation of observed surge. The RMS is calculated between the surge from

the fully nudged experiments and from observations. As in Fig. 4.6, the RMS is normalized with the standard deviation of the observed surge. The parameters L and α (Eq. 3.9) are first kept the same as for ABE, WHI and CRO (the curve N6U in Fig. 4.7). The experiment N6U is only marginally better than the CTL experiment and poorer than the ABE and WHI experiments. One would expect a better description of sea level height when more information of observed sea level height is fed into the model. However, only minor changes are seen in the ABE and WHI experiments for the German and Norwegian tide gauges. A reason for this might be that some tide gauges are located in close proximity and influence each other. Another reason that the model had difficulties reproducing the observed water levels in the English Channel in which tide gauges in the fully nudged experiments are nudged with the model.

The sensitivity of the results has, until now, been investigated with the parameters L and α being $L = 60$ and $\alpha = 1.0$. It is now elaborated on the effect of a varying α ($\alpha = 1.0$ $\alpha = 0.9$ and $\alpha = 0.5$) and L. When several tide gauges are inside each others area of influence (chosen to 100 km in Sec. 3.2.3) the weights are interpolated. To vary the interpolated weights the decorrelation radius L is varied and $L = 30$ was chosen to test the effect of a smaller geographical area being influenced from the nudged observation. The choices for α were motivated from trusting the observations with a factor 0.5 and 0.9 to saying the observations were perfect. Generally the ratios for the different experiments in the experiments with decorrelation radius of $L = 30$ (N3U,N39 and N35) are slightly better than the ones with $L = 60$ (N6U,N69 and N65). The sensitivity of the results by varying α is less than the sensitivity of varying L, but with a tendency towards better results for the German tide gauges for $\alpha = 0.5$ when $L = 30$ km. With $L = 30$ km decorrelation radius, more emphasis is put on local effects, and these might be important for tide gauges having a bathymetry not adequately resolved in the model setup or when several tide gauges are located in close proximity and influence each other. A combination of different decorrelation radii for different tide gauges would also be a possibility, but this possibility is not investigated in this thesis.

The relative errors for ABE and WHI in Fig. 4.6 have about the same magnitudes as the experiments with lowest relative errors in Fig. 4.7. Thus, most of the improvement was achieved by nudging a single tide gauge like Aberdeen or Whitby. Nudging only one tide gauge is computationally more economic and consequently was the adopted approach in this thesis. As only minor changes in the results were seen by varying the nudging coefficient, $\alpha = 1.0$ was adopted. When nudging only one tide gauge this appears to be the most reasonable choice. From the experiments with a single tide gauge

nudged, the WHI were also set up with $L = 30$ km (not shown). This did not reveal a significant difference from the experiment with $L = 60$ km. For the CRO experiment, in which poor results were achieved with $L = 60$ km, tests were made with $L = 30$ km (not shown) but only small differences were seen. From this it can be concluded that nudging Aberdeen or Whitby with $\alpha = 1.0$ and $L = 60$ seems reasonable. Due to a long available observation record from Aberdeen and promising results from Weisse and Plüß (2005) when observations from Aberdeen were combined with an ocean model, nudging Aberdeen with the multi-decadal hindcast was chosen for further analysis in this thesis.

4.2.3 Section summary

It was found that simulation of storm surge statistics improved considerably for the validation tide gauges when data from one or more British tide gauges have been nudged into the model. The improvement is most obvious for the German tide gauges and negligible for the Norwegian ones. Most improvement was obtained when only data from one British tide gauge have been nudged, and additional tide gauges in the nudging process had only minor effects. This finding may have two important consequences for operational storm surge modeling: First, when data from a tide gauge as upstream as possible are nudged, the lead time for warnings would be largest. In addition, large improvement for most of the coastal areas can be expected. Second, in the case when data from a particular station are not available in real-time, this station can be replaced by another one without having major consequences on the quality of the expected results.

Due to these findings and a relatively good availability of measurements, the tide gauge Aberdeen is used later in the thesis. The tide gauge is situated in the Northeast of UK in relative proximity to the northern open boundary.

4.3 Effect on extreme events from nudging

Hindcasts are effective means of creating a high resolved and homogeneous set of data and have been proven valuable on multi decadal time-scales (e.g., Flather et al. 1998). By combining observed values with a model simulation, information about variables that have either not been observed directly, or that have been sampled only insufficiently in space and time is provided. Additionally such a hindcast provides an improved representation of the observed natural variability. Sec. 4.2.3 suggested Aberdeen as a suitable single tide gauge to nudge. In this section results from a hindcast from 1958 to 2001, with and without observations at Aberdeen nudged, will be presented. For simplicity, the notation from Sec. 3.2.3 with CTL and ABE is maintained, as the only difference is the extension of the analysis period. The hindcast is compared with available tide gauge observations for the entire hindcast in Sec. 4.3.1. A two dimensional overview of the extreme events and the effect from nudging Aberdeen in the hindcast is presented for the whole North Sea in Sec. 4.3.2.

4.3.1 Comparison with observations

The years 1966 and 1984, the time periods 1959-1964 and 1975-1979 as well as shorter intra-annual time periods are missing in the observations taken at Aberdeen. The number of yearly available observations for this thesis for Aberdeen is shown in Fig. 4.8. The effect of the previously nudged observations stays in the model for about 0-24 hours depending on the distance from Aberdeen. After that period the ABE and the CTL experiments proximate the same values for the whole model area. To ensure comparability between CTL and ABE data -2 hours and $+24$ hours from a missing observation at Aberdeen are removed from the analysis.

For the recent years most tide gauges have a well working sampling system and the availability of data is good. With exception of Aberdeen, Cuxhaven and Borkum, none of the other tide gauges had available hourly observations to be used in this thesis previous to 1990. The total number of available hourly observations from 1958 until 2001 for each tide gauge is plotted in Fig. 4.9.

The normalized RMS between ABE and observations was shown in Sec. 4.2.2 for the time period 2000-2001. The same exercise was performed on the 44 year hindcast with available observations, and the result was very similar to ABE in Fig. 4.6 (not shown). Calculated from all hourly values

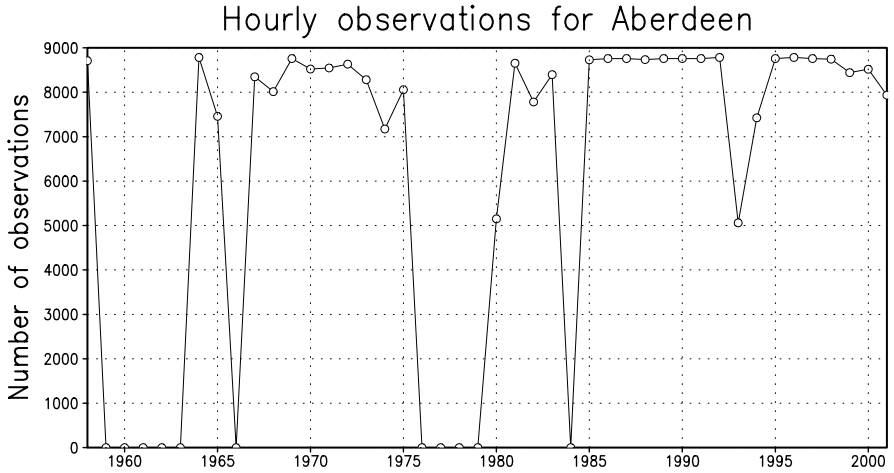

Figure 4.8: Yearly number of hourly observations for the UK tide gauge Aberdeen. Missing values for Aberdeen are filtered out in the Figs. to enable comparison between CTL and ABE.

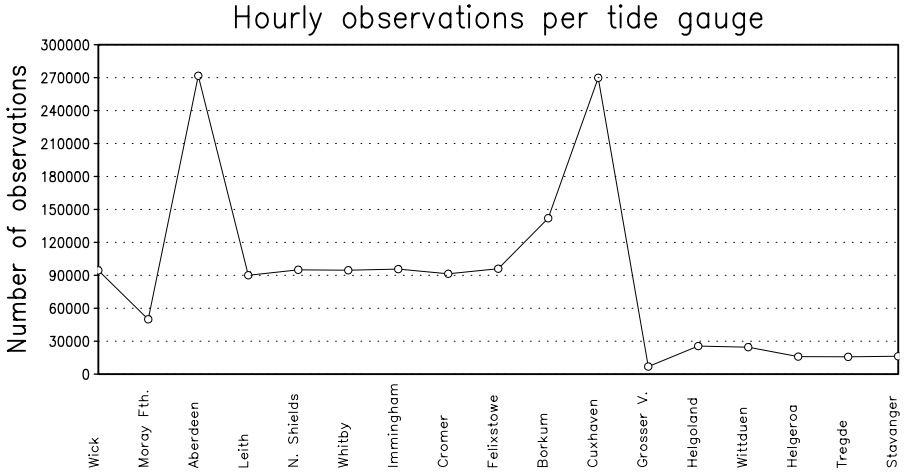

Figure 4.9: Number of hourly observations for each tide gauge available for this thesis for the time period 1958-2001.

of sea level height, correlation (upper panel in Fig. 4.10) can be taken as a measure how good the model is able to reproduce the phase of the tidal signal. As the sampling time of an hour is relatively much smaller than the tidal period, the correlation will always be high if the tide is well reproduced in the model. The largest improvement is achieved when the correlation for CTL is poorest. This is especially the case for the tide gauges in the inner parts of the German Bight and the Norwegian tide gauges, which are closer to the boundary.

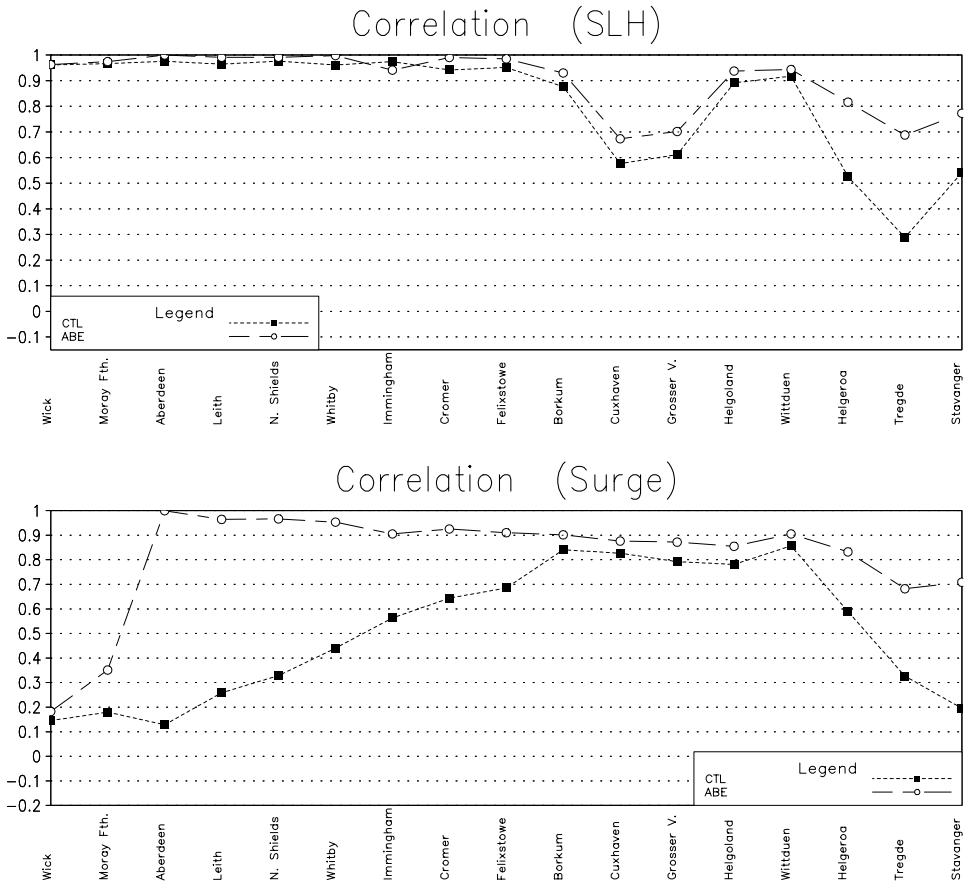

Figure 4.10: Correlation between observations and CTL and ABE for all available observations for each tide gauge. Upper panel is for SLH and lower for surge.

For surge, the correlation in the lower panel of Fig. 4.10 is always higher for the ABE experiment than for the control simulation. The tide gauge Aberdeen has a correlation coefficient of 1, and the correlation decreases with the spatial distance away from Aberdeen along the North Sea coast. The correlation for surge represents how well the surges are modeled as no tidal signal is present, contrary to the correlation for sea level height in which mostly the model's ability of reproducing the correct phase is reflected. The correlation for surge from the CTL experiment is better in the German Bight than the other tide gauges in the same experiment. This supports the hypothesis discussed in Sec. 4.2.1, that the model describes the surge better in the German Bight, which is relatively shallow and has a large spatial distance to the open boundaries.

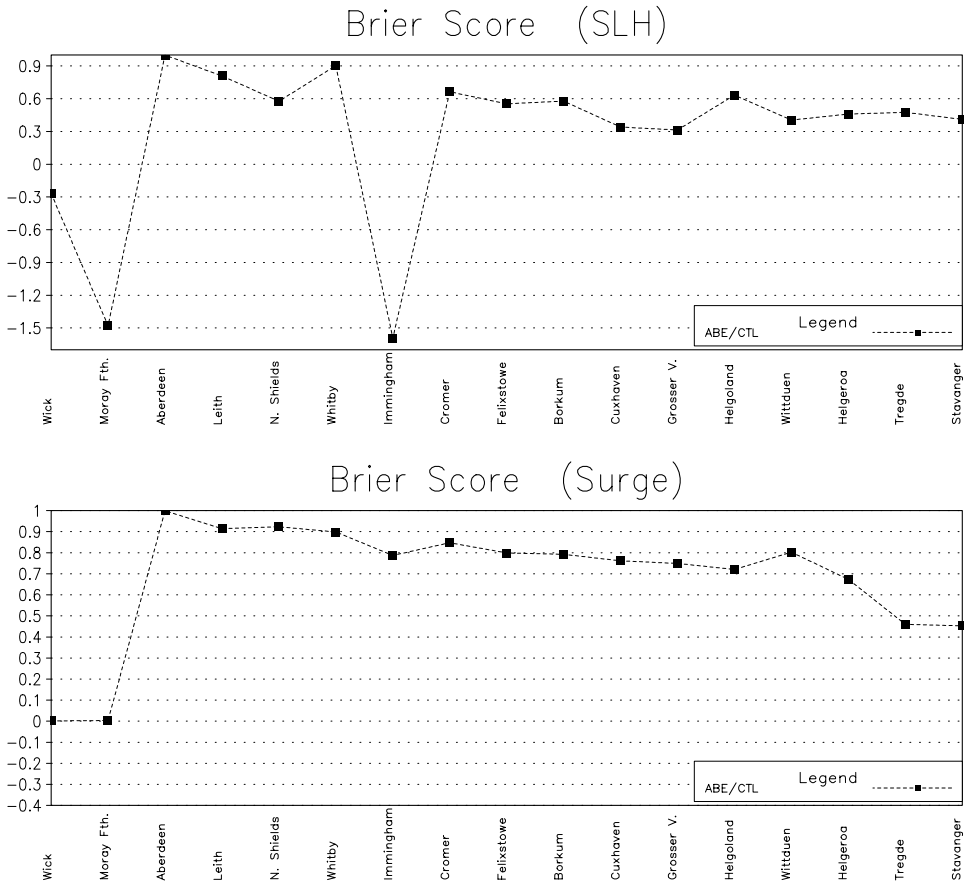

Figure 4.11: Brier score between ABE and CTL with respect to available observations for each tide gauge. Upper panel is for SLH and lower for surge.

A common way of describing the skill of quantitative forecasts, is to use a Brier skill score. The Brier skill score is a measure of the skill of the forecast F relative to a reference forecast R of the same predictand P. The comparison is made on basis of the mean-square-error S^2 of the individual forecasts, and the Brier score is given by $B_{FRP} = 1 - \frac{S^2_{FP}}{S^2_{RP}}$. Applied to the experiments in this thesis, the skill of the ABE experiment (F) relative to CTL experiment (R) is sought, and the observed values (P) are used as predictand. Positive Brier scores indicate improvement from the CTL experiment when observations from Aberdeen are nudged, and a score of 1.0 is said to be 100% improvement. Negative scores on the other hand indicate a worsening.

The upper panel of Fig. 4.11 shows that downstream of Aberdeen for all tide gauges, with exception of the tide gauge Immingham, improvement in the

modeled sea level height from CTL is achieved in the ABE experiment. For the German and Norwegian validation tide gauges a major improvement of 30-60% is achieved. The large improvement for Whitby, when Aberdeen is nudged, supports the similar results in Sec. 4.2.2 when only Whitby or Aberdeen was nudged. Fig. 4.11 also reveals, as expected, a 100% improvement for the nudged tide gauge Aberdeen where the modeled values are replaced with observed ones. The poorer result for Immingham might be explained from its geographical location in a northwest-wards bay (Fig. 3.2). Poorer results are also seen upstream of Aberdeen, but this is expected due to the fact that the tidal signal propagates downstream.

The Brier score for surge is shown in the lower panel of Fig. 4.11. Downstream of Aberdeen the ABE experiment improves the CTL by about 50-90%. The German tide gauges are considerably improved by 70-80%. The improvement decreases along the coastline with the distance away from Aberdeen. The same feature was also seen for the correlation between observed and modeled surge in the lower panel of Fig. 4.10, in which the correlation coefficient decreased from Aberdeen downstream along the coastline. Thus, a major improvement is achieved for surge for the investigated tide gauges when Aberdeen is nudged.

To this point, statistics on all data have been performed, but this does not reveal anything about the distribution of modeled and observed sea level height and surge. A common way of illustrating the distributions of two sets of data is to make a Quantile-Quantiles (QQ) plot (e.g., von Storch and Zwiers 1999). Percentiles from ABE and CTL are plotted against the observations and if they stemmed from the same distribution they would all lay on the diagonal line $y = x$. Such a method reveals the ability of nudging to improve the representation of the observed frequency distribution. Additionally a QQ-plot illustrates the differences from the CTL experiment in the frequency distribution by applying nudging. QQ-plots for sea level height did not reveal a considerably difference between ABE and CTL with respect to the observations, although generally a small improvement for ABE from CTL, at least for high percentiles, was found (not shown).

For surge, the differences in the frequency distributions between observations and the ABE and CTL experiments are larger, as shown for the UK tide gauges in Fig. 4.12 and for the German and Norwegian tide gauges in Fig. 4.13. The percentiles in the experiments are plotted against the percentiles from the observations. Generally the frequency distributions of surge in both Fig. 4.12 and Fig. 4.13 are closest to the observed frequency distribution for the ABE experiment. The largest improvements are normally seen for the highest percentiles.

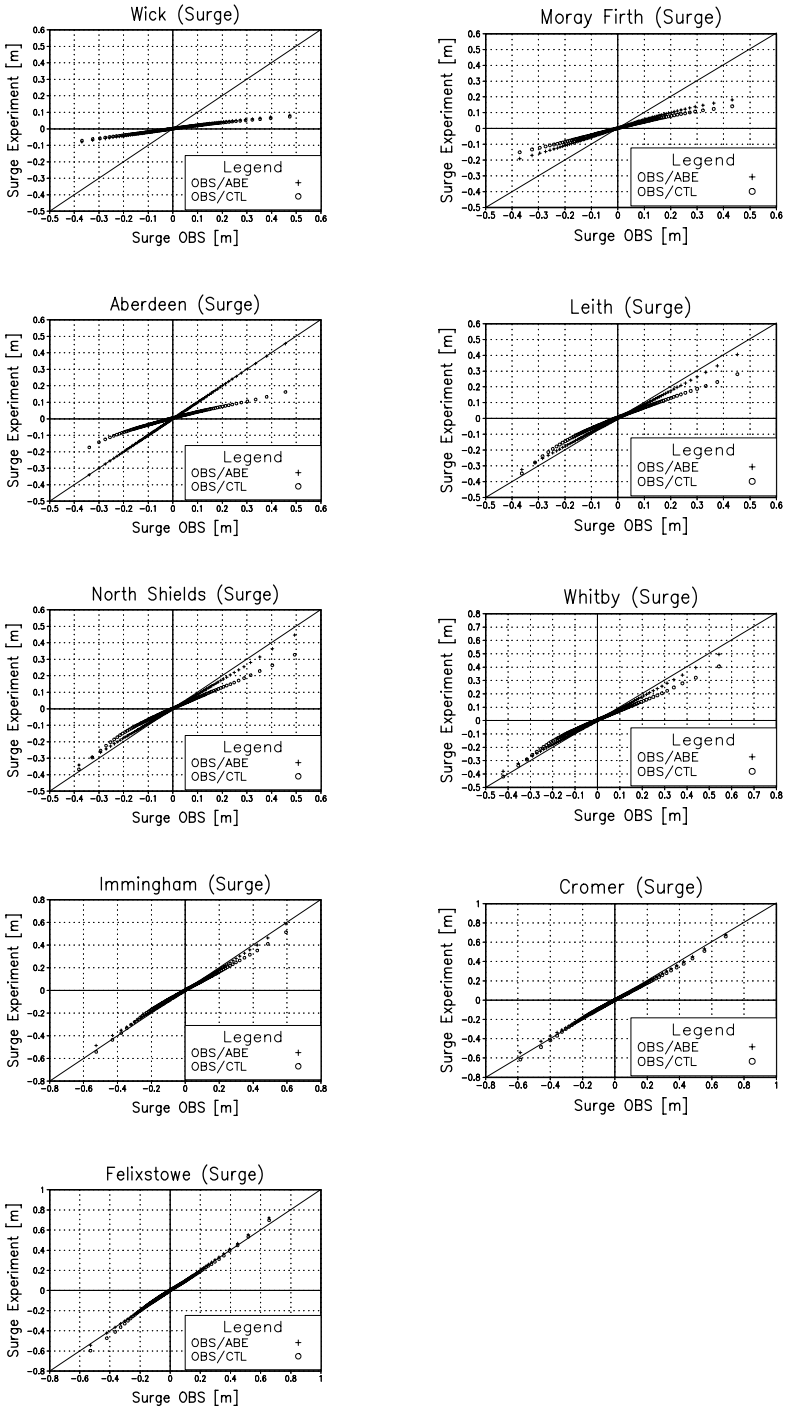

Figure 4.12: Quantile-Quantiles plot of observed and modeled surge for the UK tide gauges.
Crosses: OBS vs ABE; open circles: OBS vs CTL

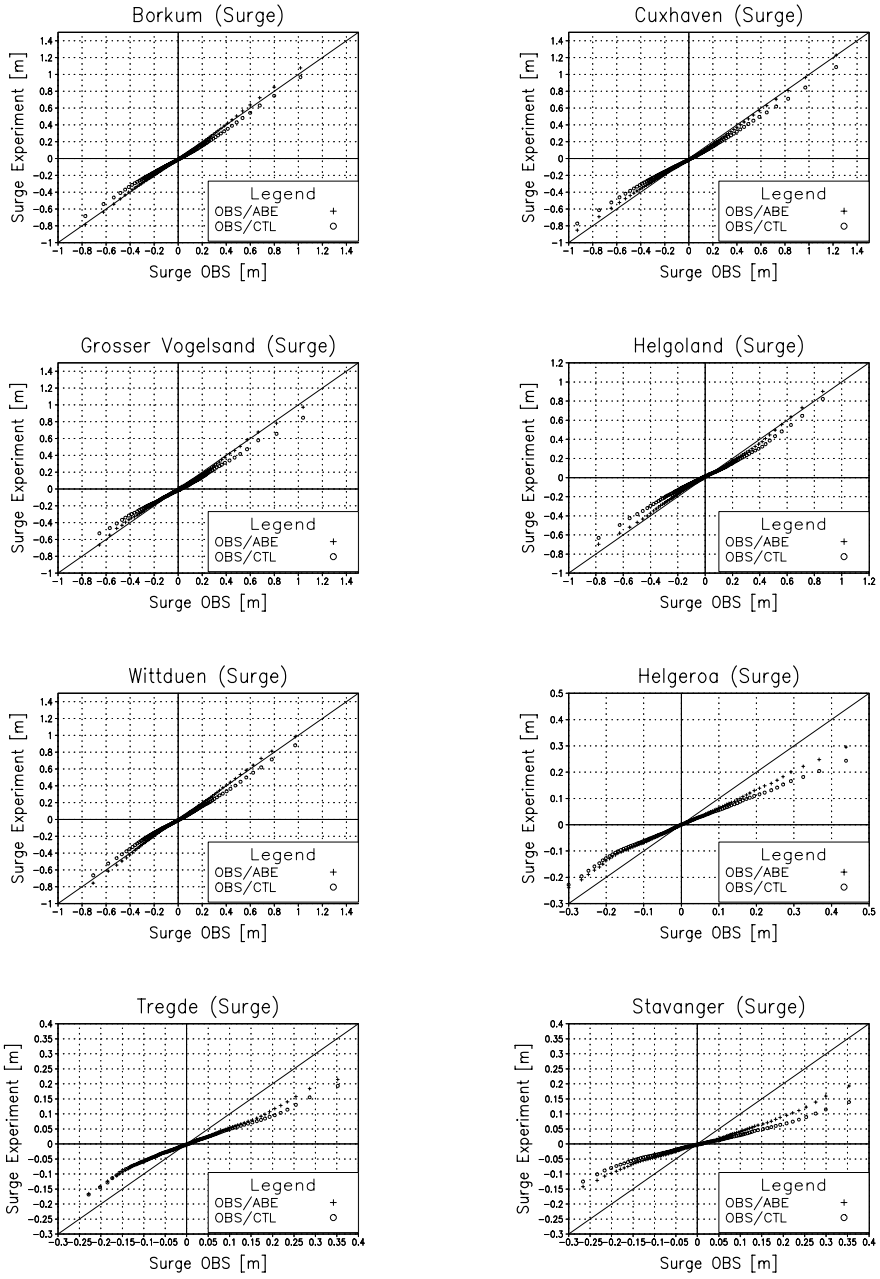

Figure 4.13: Quantile-Quantiles plot of observed and modeled surge for the German and Norwegian tide gauges.
Crosses: OBS vs ABE; open circles: OBS vs CTL

The frequency distributions in Fig. 4.12 for tide gauges downstream of Aberdeen have all widened after nudging. The distribution for Aberdeen is on

the diagonal line $y = x$ because the observed values are nudged with the model with $\alpha = 1.0$. In Sec. 4.2.1 it was noted that the modeled surge in the CTL experiment was underestimated with respect to the observed surge. This can also be seen from the frequency distributions for the tide gauges Wick, Moray Firth and Aberdeen in Fig. 4.12. The distributions from the CTL experiment are too narrow for these three tide gauges but widens for tide gauges further downstream. For Aberdeen the highest percentile in the CTL experiment reproduce only 30% of the observed value for the same percentile. The too narrow distribution is also seen in the ABE experiment for Wick and Moray Firth, as should be expected, due to the geographical location upstream of the nudged tide gauge Aberdeen. The distributions for these tide gauges are rather similar in the CTL and ABE experiments.

For the German tide gauges in Fig. 4.13, the frequency distribution has widened after nudging. The distribution of the CTL experiment is generally closer to the observed distribution for the German tide gauges than for the Norwegian and most of the British in Fig. 4.12. This is expected from the previous results of surge in which the CTL experiment was also better described for tide gauges in the German Bight. The distribution of surge in CTL is generally a straight line for all tide gauges, with exceptions of the Norwegian tide gauges, but the magnitudes are too low. The Norwegian tide gauges are have a S-form in the QQ plot, indicating that the model is not adequately reproducing the observed frequency distribution for these tide gauges.

For the ABE experiment, most tide gauges in Figs. 4.12-4.13 demonstrate a large improvement for the highest percentiles and many, some improvement for the lowest. However, it should be noted that generally the improvement in ABE from CTL relative to the magnitude of the observations is relatively constant. A possible explanation might be that external effects such as external surges, which affect the water level in the North Sea and which are contained in the observations at Aberdeen, are not accounted for in CTL.

4.3.2 Sensitivity of extreme sea level statistics by nudging

A large improvement is found in ABE compared to the CTL simulation at tide gauges downstream of Aberdeen. It can be assumed that this improvement also is representative for the whole model area and an improved description of the whole North Sea can be achieved. For coastal areas, extreme water levels are most important because of the danger of flooding and its consequences for the coastal population. To investigate extreme sea level height, the 5th and 95th percentile are chosen and presented in Fig. 4.14.

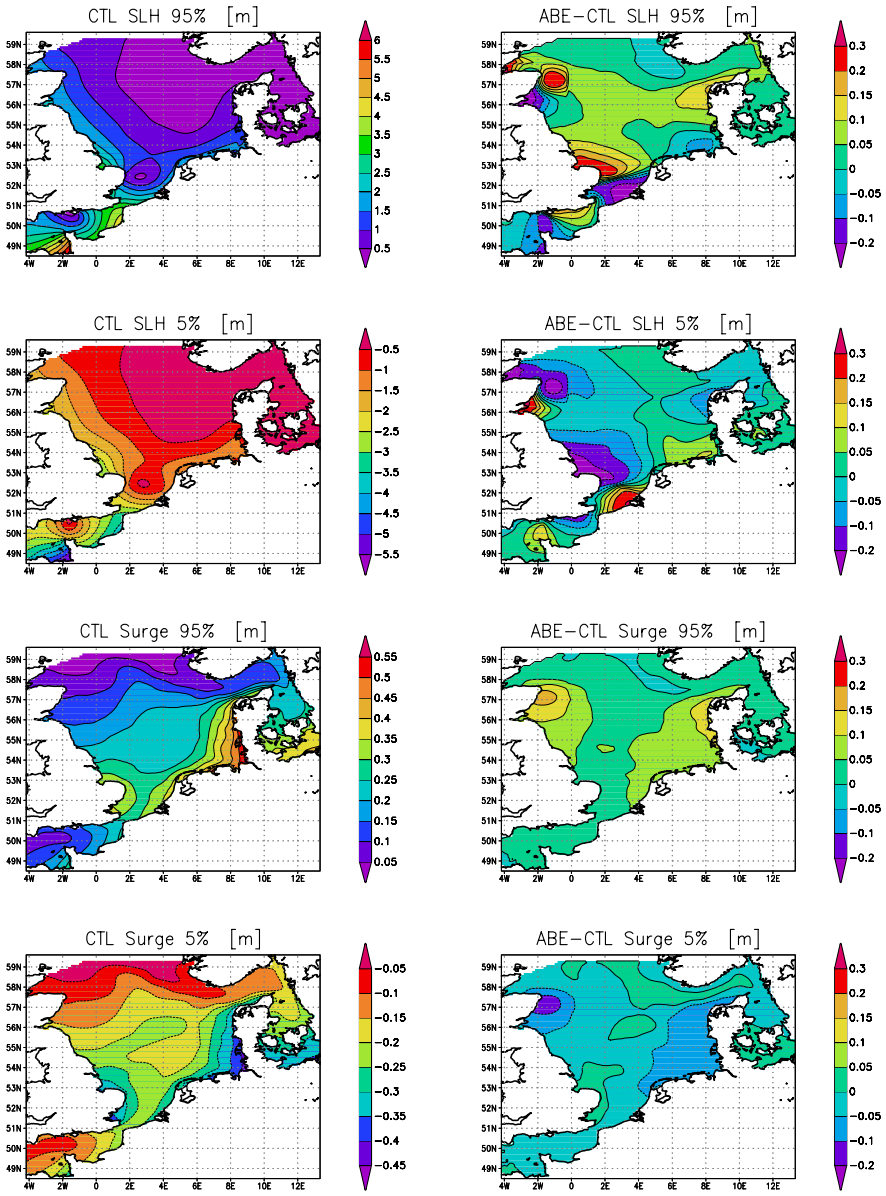

Figure 4.14: The yearly 95th and 5th percentiles averaged for all 44 years of the hindcast.
Left column: 95th and 5th percentile calculated from CTL experiment.
Right column: Difference between percentiles calculated from ABE and CTL experiments.
The first two rows are percentiles calculated from SLH and the last two from surge.
The color intervals and magnitudes in the plots on the left side are varying.

In the left column the mentioned percentiles of sea level height and surge in CTL are presented. The two first rows of Fig. 4.14 represent sea level height and the last two surge.

For sea level height in the CTL experiment (first two rows in Fig. 4.14) the spatial pattern of the percentiles have clear similarities with the standard deviation of the CTL experiment in Fig 4.2. This can be expected as extreme sea level values are an important part of the variability and because both the 50th percentile and mean sea level can be assumed to be close to zero as anomalies are used in the model.

Surge (last two rows in Fig. 4.14) has largest values for the 95th percentile (0.5 m) and small values for the 5th percentile (-0.4 m) in the German Bight and the West coast of Jutland. It is important to note that when observations are missing for Aberdeen or the investigated tide gauge, then the modeled and observed values are undefined. This enables a fair comparison between the ABE and CTL experiment but will lead to the number of observations or modeled values larger than the 95th percentile not always being the same number. Differences in the percentiles can then by created from e.g. observations of sea levels systematically missing in a season or an increased tidal range.

From a year with 365 days, hourly samplings and no missing observations the 95th percentile is the 8322nd largest value of 8760, meaning that 438 water levels higher than the 95th percentile are observed. This suggests the 95th percentile is perhaps not always representative of the extreme. To this extent, the 99th percentile was calculated (not shown). The spatial pattern for the 99th percentile looks very similar to 4.14 for both sea level height and surge but with a larger magnitude of modeled sea level height. Largest differences are for the surge values in the German Bight, which are up to 1 m, contra 0.5 m for the 95th percentile.

The right column of Fig. 4.14 shows the difference between ABE and CTL for the different percentiles calculated from sea level height and surge. The impact of nudging is, for all plots, seen in close proximity to Aberdeen. For sea level height (first two rows of Fig. 4.14) a difference between ABE and CTL is seen at the Southeast coast of UK, which is roughly half a period of the M_2 tidal constituent away from Aberdeen, and in the German Bight (one period of M_2).

In addition to the differences close to Aberdeen, for surge (last two rows of Fig. 4.14) the main effect of nudging is observed in the German Bight and on the West coast of Jutland. The CTL experiment in the left column of

Fig. 4.14 also had largest values for the 95th percentile and the smallest for the 5th percentile for the same areas. It can be concluded that an increase for the 95th percentile of 8-12 cm and a decrease for the 5th percentile is achieved after nudging. When the percentiles were compared with observations generally an improvement was seen in the ABE experiment compared to the CTL simulation. For this reason it is interesting to investigate the effect from nudging on long-term changes and inter-annual variability of the extreme water levels presented in this section; undertaken in Sec. 4.4.

4.3.3 Section summary

A multi-decadal hindcast with the regional ocean model TRIMGEO combined with observational sea level data from Aberdeen was performed for the 44 year time period 1958-2001. Model and data were combined utilizing a simple but cost-effective nudging scheme.

It was shown that the nudging method improves the modeled sea level height for the simulation period and the largest improvements are for the surge. The RMS for surge for the German tide gauges were reduced by 70-80%. Additionally the nudging method is effective in widening the modeled distribution of surge towards the observed distribution for the tide gauges close to northern open boundary.

The reduced RMS is probably due to external effects, such as external surges, which are taken into account in the ABE experiment by nudging observations from Aberdeen. The remaining differences in the observed values are likely to be non-meteorological effects not included in the model setup. Such effects could be changes in the bathymetry by e.g. construction works (e.g. dredging, embankments) or natural morphodynamical processes, a rise in mean sea level or land rising/sinking.

The largest changes after nudging, in addition to close proximity of the nudged tide gauge Aberdeen, are observed in the German Bight and on the West coast of Denmark. For surge an increase of 8-12 cm from the CTL experiment is achieved for the 95th percentile after nudging. As the investigated tide gauges showed an improvement from the CTL experiment after nudging Aberdeen, these values are assumed to be an improvement from the CTL experiment, in which no nudging was applied.

The improved hindcast with nudging applied is valuable as an improved high-resolved data set, and extreme values investigated in this section will be further elaborated with respect to long-term changes and inter-annual variability in Sec. 4.4.

4.4 Long-term changes and variability of extreme events

Sec. 4.3 focused on the time-average conditions of a multi-decadal hindcast combined with observations from Aberdeen. Here the inter-annual variability and long-term changes of trends are discussed. The emphasis is on differences between the CTL and ABE simulation. First, observed annual and seasonal extremes and their trends from tide gauges in the German Bight with relatively long observational records are compared to the ABE and CTL hindcasts. Second, a two dimensional view of the differences between the two simulations is presented.

4.4.1 Comparison with observations

The previous section focused on extremes derived from hourly values. In this section the focus set on annual and seasonal high (HW) and low waters (LW). This was motivated from additional observations in which only observed high and low waters were available. The model data is transformed to high and low waters, and this transformation may create small discrepancies in the timing and magnitude of the high and low waters if e.g. the model sampling appears on both sides of a maximum or minimum. These discrepancies in timing and magnitude, however, are neglected in the analysis.

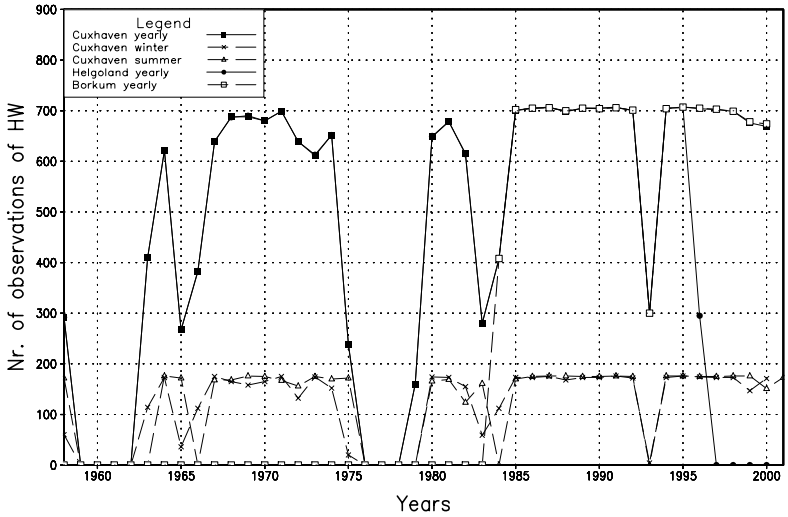

Figure 4.15: Number of yearly high waters for the tide gauges and seasons further investigated in this thesis.

Fig. 4.9 showed the hourly observations available for this thesis. Three of the tide gauges with the longest observational record available for this thesis were the German Bight tide gauges Cuxhaven (1958-2001), Helgoland (1958-1996) and Borkum (1985-2001). These tide gauges are all located in the German Bight and have a large spatial distance to the nudged tide gauge Aberdeen. Therefore, Borkum, Helgoland and Cuxhaven are used to compare long-term changes from CTL and ABE with the observed ones. Data for Helgoland were already available for HW/LW, the data for Cuxhaven and Borkum were transformed from hourly data to HW/LW the same way as the respective model values in the experiments.

As previously, time steps when Aberdeen is missing (Fig. 4.8) are removed -2 hours and $+24$ hours from the missing observation in the statistics to be able to estimate the differences of the CTL and ABE experiment coming from the nudging approach. For Helgoland a different approach was adopted because the observations were already available for high and low waters. The observed high or low water at Helgoland was checked for a missing observation at Aberdeen 0-24 hours in the past. If a lack is found, the observed high or low water at Helgoland is rejected from the analysis. The resulting number of observations are shown in Fig. 4.15. When the tide gauges had a similar number of available observations, the curves in Fig. 4.15 become difficult to separate.

4.4.1.1 Cuxhaven

The tide gauge Cuxhaven is a German tide gauge with a long historical observational record and it was established in 1784 (Siefert, 1970). Additionally, the geographical location of Cuxhaven is important because of the large, flat and heavily populated land areas close to the coastline. Cuxhaven is also a well investigated tide gauge by e.g., Jensen et al. (1988) and Gönnert (2003). An improvement after nudging was observed in Sec. 4.3 for the 44 year statistics based on hourly values. In this section it will be determined if an improvement in long-term changes and inter-annual variability of high and low waters can be achieved by nudging.

In Fig. 4.16 annual mean high (anMHW) and low water (anMLW), tidal ranges (anMTR) (calculated as $\overline{HW - LW}$) and upper and lower percentiles from observations and the ABE and CTL simulation are compared. In general, there is a rather good agreement and the year-to-year fluctuations are captured remarkably well. However, there remain different biases for the different parameters. For annual mean high water, the bias has been reduced by about 9 cm compared to the control simulation leading to an improved representation of high waters in the ABE simulation.

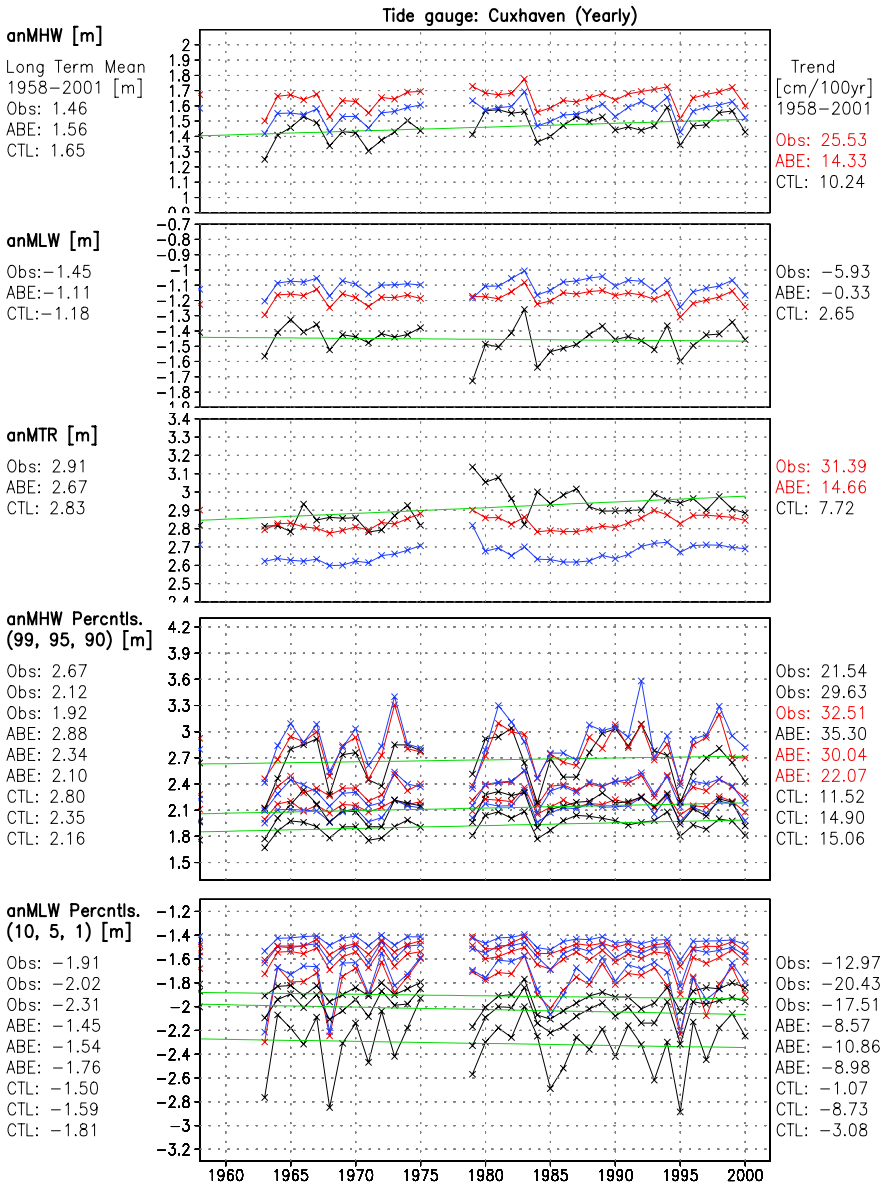

Figure 4.16: Yearly statistics for CTL experiment (red), ABE experiment (blue) and observed (black) for the tide gauge Cuxhaven. From top to bottom: annual mean high water (anMHW), annual mean low water (anMLW), annual mean tidal range (anMTR), 99th, 95th and 90th percentile of annual high waters and 10th, 5th and 1st percentile of annual low waters. Mean values are listed left and linear trends on the right and both in the same order as the percentiles for the bottom two rows. Red numbers mean trends are significantly different from zero at a 95% confidence level. Green lines are the observed trend.

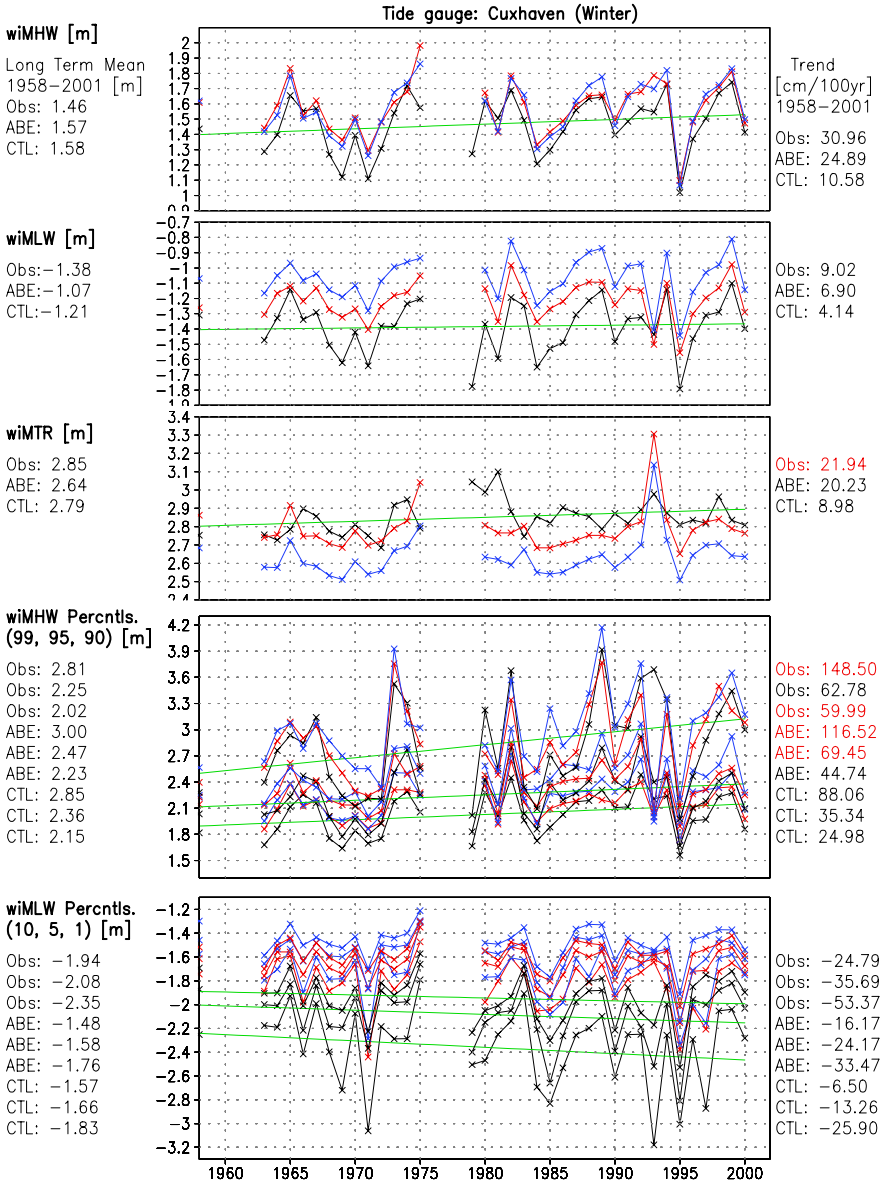

Figure 4.17: Statistics for the winter months (DJF)for CTL experiment (red), ABE experiment (blue) and observed (black) for the tide gauge Cuxhaven. From top to bottom: winter mean high water (wiMHW), winter mean low water (wiMLW), winter mean tidal range (wiMTR), 99th, 95th and 90th percentile of winter high waters and 10th, 5th and 1st percentile of winter low waters. Mean values are listed left and linear trends on the right and both in the same order as the percentiles for the bottom two rows. Red numbers mean trends are significantly different from zero at a 95% confidence level. Green lines are the observed trend.

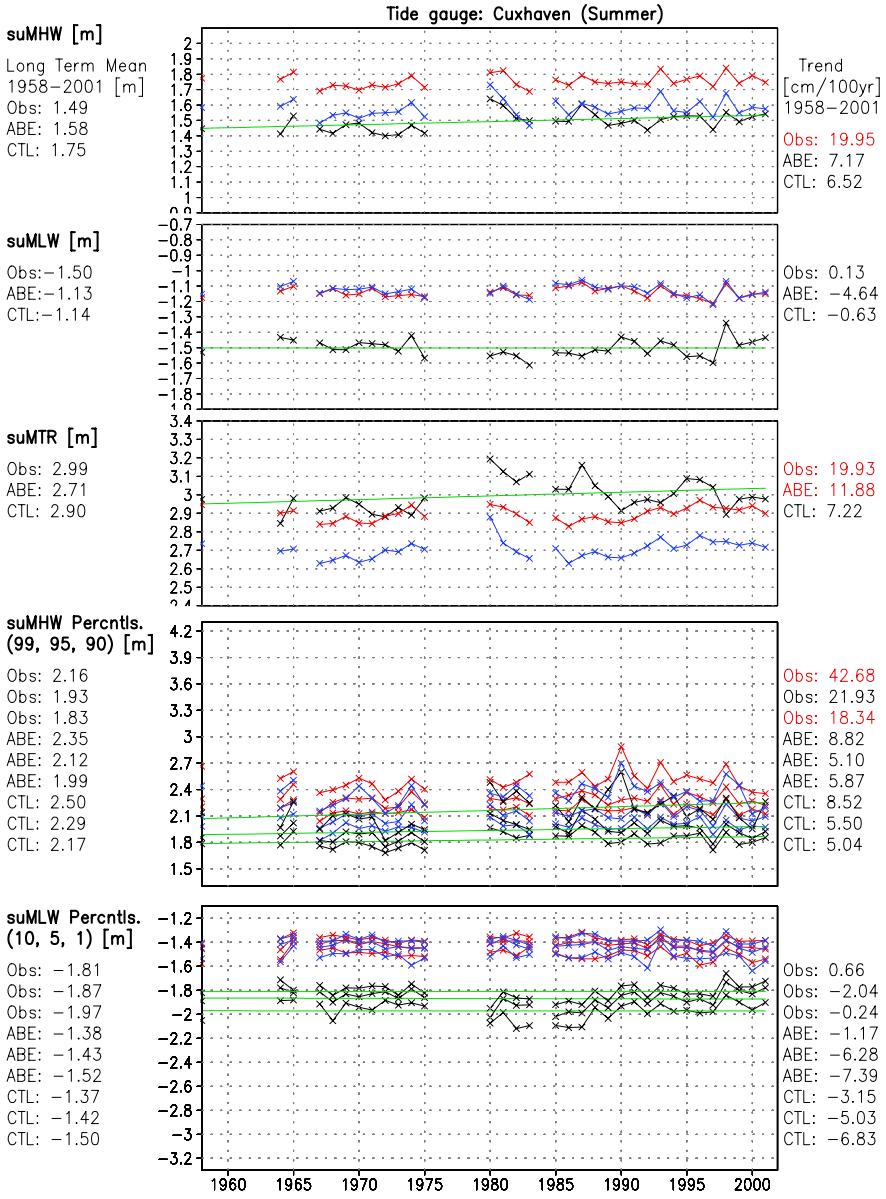

Figure 4.18: Statistics for the summer months (JJA) for CTL experiment (red), ABE experiment (blue) and observed (black) for the tide gauge Cuxhaven. From top to bottom: summer mean high water (suMHW), summer mean low water (suMLW), summer mean tidal range (suMTR), 99th, 95th and 90th percentile of summer high waters and 10th, 5th and 1st percentile of summer low waters. Mean values are listed left and linear trends on the right and both in the same order as the percentiles for the bottom two rows. Red numbers mean trends are significantly different from zero at a 95% confidence level. Green lines are the observed trend.

The quality of the representation of low waters and tidal ranges have, however, slightly decreased through the nudging of Aberdeen data. A similar conclusion can be drawn from long-term means of the upper and lower percentiles, with exception of the 99th percentile (Fig. 4.16). Summarizing, the improved representation of high water characteristics in the ABE run is at a cost of a higher bias in the low water characteristics. It should be noted, however, that the latter is not very well reproduced neither in the ABE nor in the CTL run.

Cuxhaven is located in an area with relatively shallow water. Consequently, the model might have problems describing the tide for Cuxhaven in the spatial resolution of $\frac{1}{6} \times \frac{1}{10}$ degree because of complicated bathymetry and shallow water. This matter was further examined by performing a simulation with no meteorological forcings included (tide-only). Analysis of this simulation confirmed a positive bias existing in the model also when no meteorological forcings were applied. Additionally one has to remember that comparing a mean value of a model grid box of about 10x10 km might not be a fully comparable value to point observations taken at one specific location. This will always make a direct comparison of a numerical model with observed data difficult as long as the model does not have a very high resolution. A common problem for low waters in a coarse model resolution is land left dry due to the retreating water masses. This dry land is not "seen" by the model and the water masses will be calculated as if the land was covered by water.

The operational model at BSH is a closely related numerical regional ocean model to TRIMGEO and used some of the same boundary values as in this thesis (Esselborn, pers. comm. 2003). For Cuxhaven, Dick et al. (2001) report a positive bias in modeled sea level height for high waters as well as low waters, with the largest bias for the latter. This result is consistent with Fig. 4.16 and supports the hypothesis that the model has a bias in modeling the observed water levels for Cuxhaven with the actual model setup.

On the right side of Fig. 4.16 the linear trends are plotted for anMHW, anMLW, anMTR and the upper and lower percentiles calculated from observations and the CTL and ABE experiment. All trends are closer to the observed trends in the ABE experiment than in the CTL experiment, with the exception of the trend for the 99th percentile.

The CTL and ABE experiment are both driven by the same meteorological forcings in the model area. Additionally, the ABE experiment has external processes such as external surges included in the model simulation through the nudging of observed values for the Aberdeen tide gauge. As a result

the ABE experiment generally improves the long-term statistics and inter-annual variability. However, non-meteorological effects are not accounted for in both simulations. Such non-meteorological effects being e.g., land-rise, mean sea level rise, dredging and other constructional works. A rise in sea level would have been included in the ABE experiment if the nudged sea level height for Aberdeen had been calculated from the reference level of the tide gauge. However, the yearly means were adopted as reference level in this thesis because the OD for Aberdeen was not known at the beginning of this work.

A significant positive trend for anMHW, anMTR and the 90th percentile is observed at Cuxhaven and also reproduced after nudging, however, even though the trends from the control simulation also are positive, they are smaller than the trends from the observations and ABE, and not significantly different from zero.

The other significant trend in Fig. 4.16 is for the 95th percentile in the ABE experiment, which is close to the observed trend after nudging, however the observed trend is not significantly different from zero. For the anMLW, no trends are significantly different from zero, but after nudging the trends calculated from observations and from the ABE experiment are both slightly negative. Negative trends are also observed for the lower percentiles and in both experiments, but none of them were significant.

Sec. 3.2.5 mentioned two different ways of calculating the significance of a linear trend, e.g. an auto-correlation in the timeseries can influence the calculation of the significance of trends. The largest auto-correlation was for Cuxhaven, found for the 5th and 10th percentile. The parametric test in Sec. 3.2.5 is used to calculate the significance of the trends in this thesis as the matter is further tested with and without pre-whitening, which should be used when the data have a high auto-correlation, in Sec. 4.4.2, and only small differences were found.

The fact that the improvement in Fig. 4.16 is not as considerable as was seen in Sec. 4.3.1 motivated a closer investigation of the seasonal variation of the long-term statistics. The yearly statistics was separated in an analysis period for the summer months (June, July and August) and the winter months (December, January and February).

Fig. 4.17 shows the same parameters as in Fig. 4.16 for the winter months. A reasonably good fit of the high waters in the winter is already revealed in the CTL experiment, and a visual inspection, shows a considerably better fit for the CTL experiment for winter statistics than for the yearly statistics

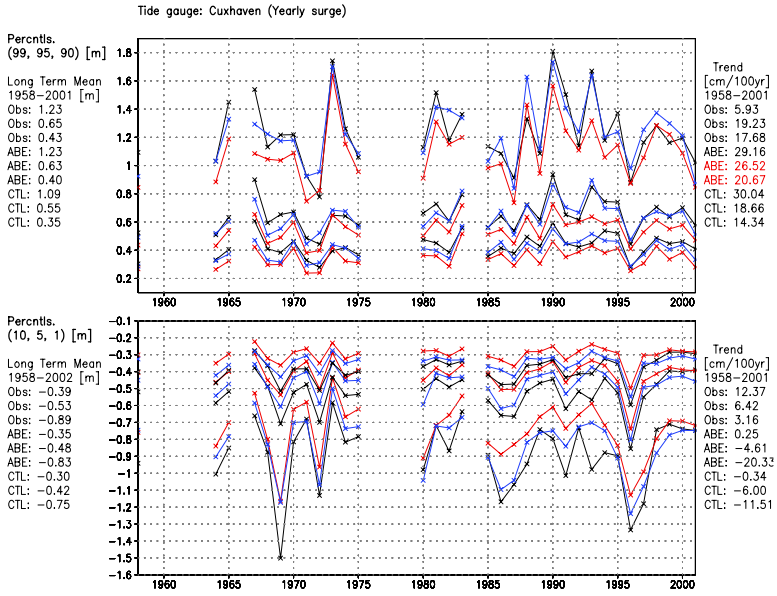

Figure 4.19: Yearly percentiles of surge values for the tide gauge Cuxhaven. Black curve is observations, red is CTL experiment and blue is ABE experiment.
Panel 1: 99th, 95th and 90th percentile.
Panel 2: 10th, 5th and 1st percentile.
Mean values in same order on the left side and linear trends on the right side. Trends in red are significantly different from zero at a 95% confidence level.

in Fig. 4.16. Also here a slight improvement is seen in the mean value for high waters after nudging, but the other long-term means are closer to those observed in the CTL run.

The winter months are the season with most storminess and most extreme events in sea level height. Generally winter statistics in Fig. 4.17 are better described than yearly statistics in Fig. 4.16. Low waters are also poorly described for the winter. Possibly, the actual model setup used in this thesis is better fitted for the high waters in the winter season when the storm surges normally are stronger and more frequent.

All trends on the right hand side in Fig. 4.17 calculated for the ABE experiment are relatively close to the observed trends. The modeled trends for the high percentiles in ABE are closer to the observed trends than the same trends in CTL, and the 95th and 90th percentile are both significantly different from zero.

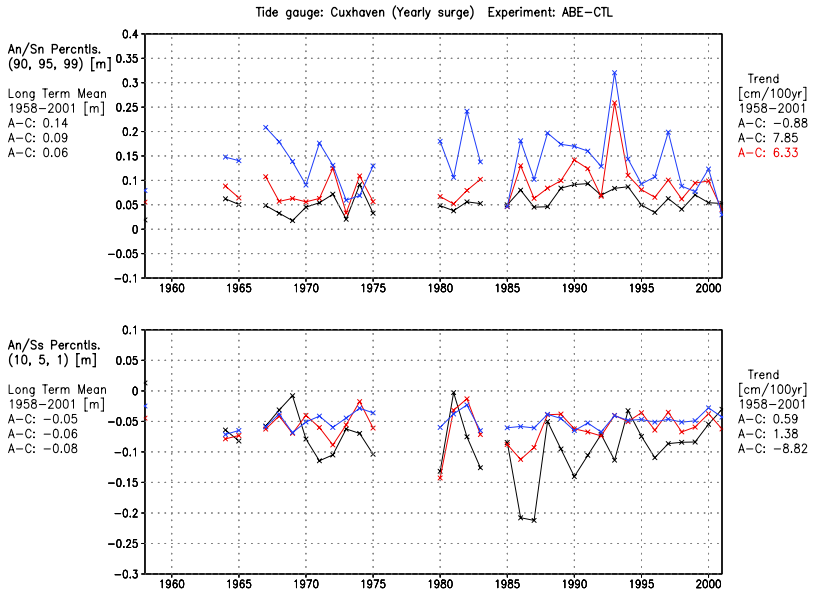

Figure 4.20: Difference between yearly percentiles for the tide gauge Cuxhaven from the ABE and CTL experiments.
Upper panel: 99th (blue), 95th (red) and 90th (black) percentiles.
Lower panel: 10th (blue), 5th (red) and 1st (black) percentiles.
Mean values in same order on the left side and linear trends on the right side. Trends in red are significantly different from zero at a 95% confidence level.

The trends calculated from winter statistics of the ABE experiment are generally closer to the observed than from the CTL experiment, and the same as was seen for yearly trends. An added value from nudging is achieved as external effects, as for example, external surges are accounted for in the observed water levels for Aberdeen. However, previously discussed non-meteorological effects are not accounted for in the normal model setups. The remaining differences between the long-term observations and the ABE simulation can be interpreted as a measure of the non-meteorological effects.

The statistics for the high waters in the winter season are closer to the observed than for the yearly statistics. Thus, is it natural also to investigate the summer months for Cuxhaven. Fig. 4.18 presents the same parameters as for the previously discussed yearly and winter statistics, when the statistics are calculated from HW/LWs during the summer. The improvement after nudging is obvious. As for the yearly and winter high waters, there is a positive bias in the high waters but the high waters are considerably closer to the observed high waters after nudging. For low waters the ABE experiment is more or less similar to CTL, and because of the improvement in high waters there is a negative bias in suMTR after nudging.

Generally only minor changes between the CTL and the ABE experiment are seen for the calculated linear trends on the right hand side of Fig. 4.18. The suMTR is an exception, the trend has increased and like the observed trend, is significantly different from zero. The observed trend for suMHW, as well as the 90th and 99th percentile, are all significantly different from zero but the modeled values are not significant and considerably smaller.

From Fig. 4.16 one can clearly see an improvement for the anMHW, however, the improvements are dependent on the season. Cuxhaven is located in the German Bight and differences in the quality of the model for summer and winter season may come from:

- Water levels being affected due to a seasonal cycle in the water stratification and stronger/weaker residual currents, which are not accounted for in a two dimensional model setup.
- Seasonal variation in the fresh water input due to a seasonal cycle in precipitation and river runoff affecting the stratification or the water levels directly.
- Seasonal shortcomings in the atmospheric forcings creating seasonally different values for the modeled surge.
- Seasonal dependency in the description of the tide at the open boundaries creating a seasonal variation of modeled sea level height from the open boundary.

The points listed above could all explain a seasonal variation in the German Bight. Huthnance (1997) reported a highly variable and a strong seasonal variation in inflow of water from the North Atlantic and through the English Channel. However, timeseries of differences between CTL and observations at Wick located almost at the northern open boundary also show a seasonal cycle and a better fit to the observations in the winter than the summer (not shown). The underestimation in the summer in close proximity to the open boundary leads to the most probable conclusion of a seasonality that is not accounted for in the boundary values for the tide at the open boundary. Such a seasonality would affect the tide gauges in the German Bight, but a combination of the other above described points can not be excluded for this area.

To this point in this section, long-term changes in sea level height have been investigated for Cuxhaven. In Sec. 4.3.1 the quantiles in Fig. 4.13 showed a clear improvement for surge after nudging. To closer investigate the long-term changes in surge, the timeseries of the 1st, 5th, 10th, 90th, 95th and

99th percentiles of surge from Cuxhaven are plotted in Fig. 4.19 for the CTL and ABE experiments.

The CTL experiment has a good visual fit with the observed year-to-year fluctuation but it systematically underestimates the surge. However, after nudging, the surge is remarkably better modeled. This was also seen for quantiles in Fig. 4.13 which consists of quantiles for all time steps. Contrary to sea level height, all long-term mean values and trends improve for surge after nudging, with exception of the trend for the 1st percentile.

The improvement after nudging is obvious for surge (Fig. 4.19) but how large is the difference between the CTL experiment and the ABE experiment in which observations are combined with the model? The differences between yearly 99th, 95th, 90th, 10th, 5th and 1st percentiles of surge from ABE and CTL are plotted in Fig. 4.20. All the high percentiles have a positive difference indicating higher percentiles in the nudged experiment. For the low percentiles it is generally a negative difference for all years with some exceptions. The largest differences are generally found for the 99th and 1st percentile.

From a visual inspection a considerably improved description of the inter-annual variability in Fig. 4.20 after nudging is revealed. To quantify the effect of nudging for surge the Brier score, which was defined in Sec. 4.3.1, could be used. A positive Brier Score would indicate an improvement in the ABE experiment from the CTL experiment and the different scores for the different percentiles in Fig. 4.19 are listed in Tab. 4.1. All percentiles are improved in the ABE experiment and the Brier scores vary from 0.58-0.80. These values are comparable to the calculated Brier score for all 44 years for Cuxhaven in Sec. 4.3, which for surge was 0.79 (Fig. 4.11).

The linear trend obtained from the 90th percentile of surge on the right hand side in Fig. 4.20 is the only significant trend. Except of the 99th and 1st, all trends of the differences between surge from ABE and CTL are positive. From this it can be concluded that the 90th percentile of surge in the ABE experiment is significantly different from the CTL experiment and the calculated Brier score for the 90th percentile is 0.71.

	Cuxhaven					
	99th	95th	90th	10th	5th	1st
Brier score	0.59	0.80	0.71	0.69	0.65	0.58

Table 4.1: Brier score for percentiles of surge at Cuxhaven. Calculated for ABE versus CTL in Fig. 4.19 with the surge calculated from observed values as the common predictand.

Summarizing, it can be concluded, that after nudging a considerable improvement can be seen in high waters for Cuxhaven but a worsening for low waters. There is also a seasonal variation in the difference between modeled and observed sea level height, and the modeled values are closer to the observed values for the winter season. For surge a much better fit of the inter-annually variability is achieved by nudging and the different percentiles from surge are improved by 58-80%.

4.4.1.2 Helgoland

The tide gauge Helgoland is located next to the island Helgoland in the German Bight and in deeper water than Cuxhaven. The tide gauge has a long observational record and available observations of HW/LW for Helgoland were provided from the BAW and were used to investigate the effect of nudging for the long-term changes of extreme events at Helgoland. On one hand the island Helgoland is surrounded by deeper water depths than Cuxhaven, on the other hand the island is quite small and not a land cell in the current resolution of TRIMGEO.

In Fig. 4.21 annual mean high (anMHW) and low water (anMLW), tidal ranges (anMTR) and upper and lover percentiles from the observations and the ABE and CTL simulations are compared for Helgoland in the same way as Fig. 4.16 for Cuxhaven. In general, similar as for Cuxhaven, the modeled values are higher than the observed ones for high waters in the CTL experiment (16 cm in average for anMHW). After nudging a slight improvement (5 cm in average for anMHW) can be seen for the high percentiles. The yearly variation of anMLW from the CTL experiment is closer to the observed variation compared to the corresponding values for Cuxhaven (5 cm vs 27 cm in average).

The observed trends on the right hand side of Fig. 4.21 for anMHW and anMTR are both significantly different from zero for Helgoland. The ABE experiment is working in a similar manner as for Cuxhaven. A clear improvement is achieved for high waters, and a worsening for low waters. In the ABE simulation all trends are considerably closer to the observed trends than in the CTL, and the long-term trends of the 95th and 90th percentiles are closest to the observed values. The trends for the same percentiles, are after nudging, also significantly different from zero.

The largest improvements for Cuxhaven occurred in the summer when the CTL experiment was differing more from the respective observed values than for the yearly observed values. A similar tendency can also be observed for

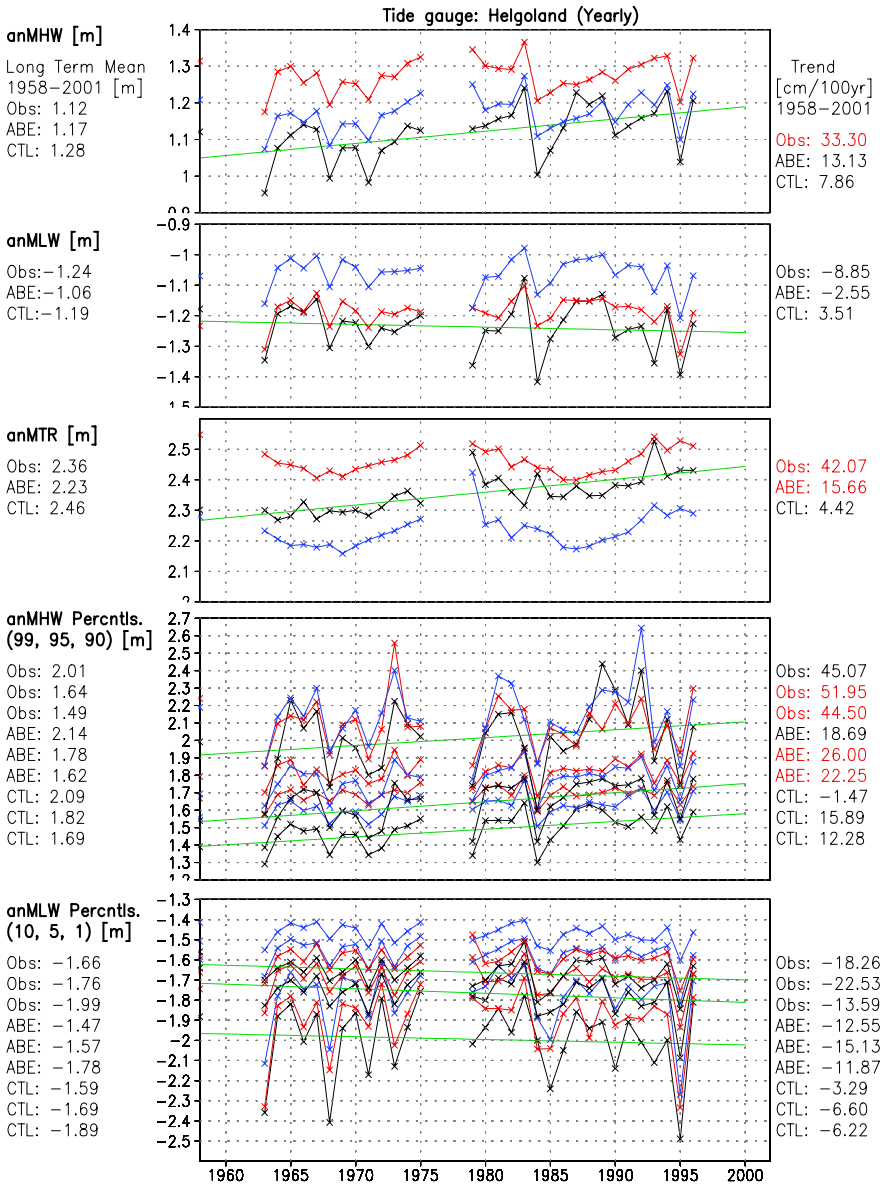

Figure 4.21: Yearly statistics for CTL experiment (red), ABE experiment (blue) and observed (black) for the tide gauge Helgoland. From top to bottom: annual mean high water (anMHW), annual mean low water (anMLW), annual mean tidal range (anMTR), 99th, 95th and 90th percentile of annual high waters and 10th, 5th and 1st percentile of annual low waters. Mean values are listed left and linear trends on the right and both in the same order as the percentiles for the bottom two rows. Red numbers mean trends are significantly different from zero at a 95% confidence level. Green lines are the observed trend.

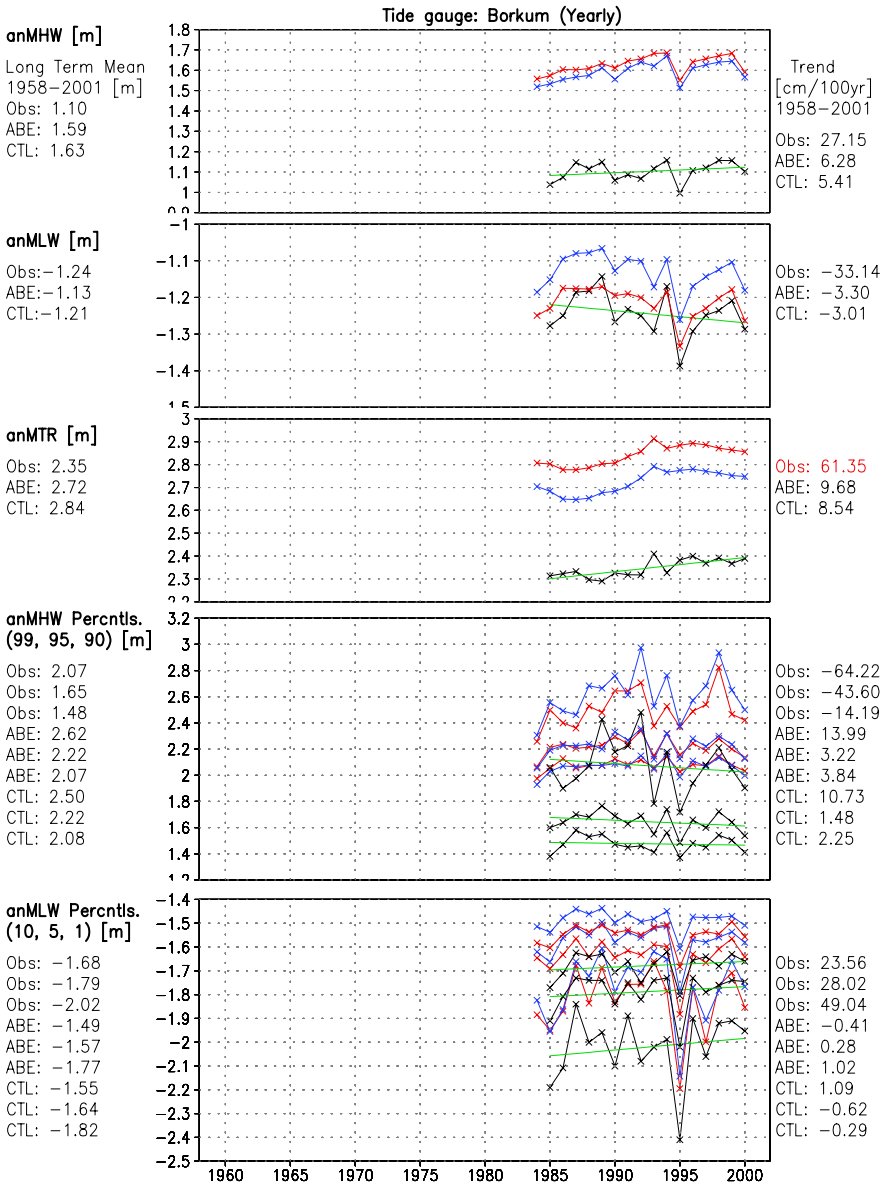

Figure 4.22: Yearly statistics for CTL experiment (red), ABE experiment (blue) and observed (black) for the tide gauge Borkum. From top to bottom: annual mean high water (anMHW), annual mean low water (anMLW), annual mean tidal range (anMTR), 99th, 95th and 90th percentile of annual high waters and 10th, 5th and 1st percentile of annual low waters. Mean values are listed left and linear trends on the right and both in the same order as the percentiles for the bottom two rows. Red numbers mean trends are significantly different from zero at a 95% confidence level. Green lines are the observed trend.

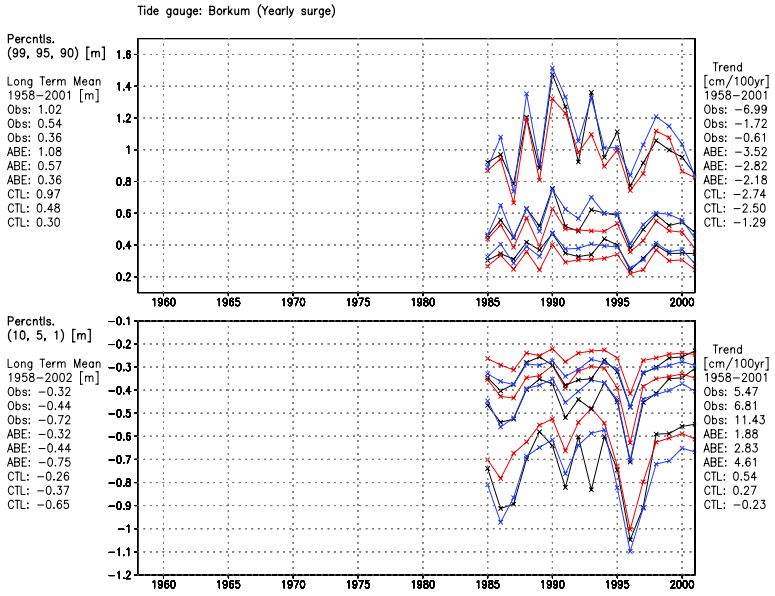

Figure 4.23: Yearly percentiles of surge values for the tide gauge Borkum. Black curve is observations, red is CTL experiment and blue is ABE experiment.
Panel 1: 99th,95th and 90th percentile.
Panel 2: 10th,5th and 1st percentile.
Mean values in same order on the left side, and linear trends on the right side. Red values for trends are significantly different from zero at a 95% confidence level.

Helgoland (not shown). Cuxhaven and Helgoland are both situated in the German Bight about 70 km apart, and both the modeled and the observed values have clear similarities. The main difference is that Cuxhaven is located at the coast within large tidal flats and Helgoland off the Wadden Sea in relatively deep water. This might be the reason why the low waters in the CTL experiment are modeled better for Helgoland than for Cuxhaven.

In the ABE experiment, the anMLW is higher than in the CTL experiment and the observations. The deeper bathymetry may explain the better modeled values in the CTL experiment, but not why the anMLW is too high after nudging. The seasonal variation of the tidal boundary conditions might be an explanation. Closer investigation of Helgoland reveals a very good fit of the anMLW as well as the anMHW for the winter, and a positive bias in the summer.

The high and low waters for the experiments for Helgoland are calculated from hourly values, however, the observations are already provided for HW/LW

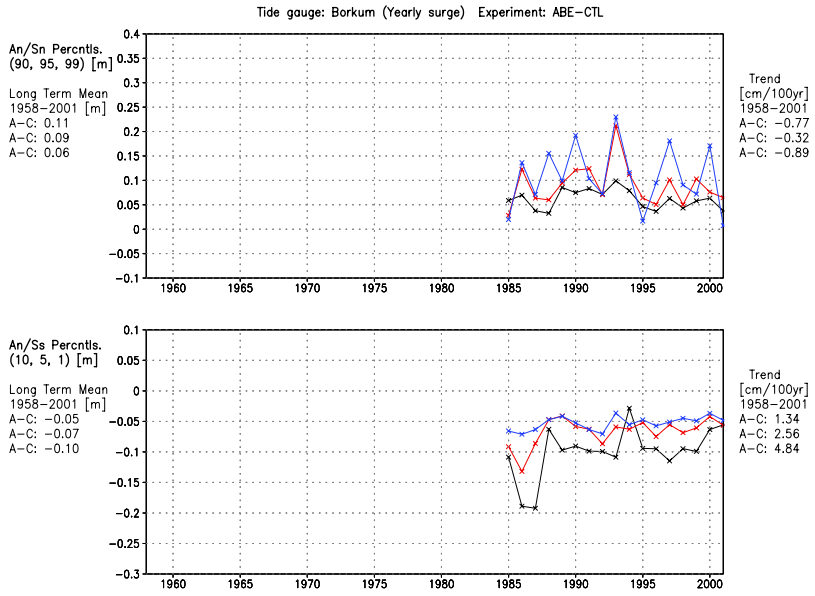

Figure 4.24: Difference between yearly percentiles for the tide gauge Borkum from the ABE and CTL experiments.
Upper panel: 99th (blue), 95th (red) and 90th (black) percentiles.
Lower panel: 10th (blue), 5th (red) and 1st (black) percentiles.
Mean values in same order on the left side, and linear trends on the right side. Red values for trends are significantly different from zero at a 95% confidence level.

with the exact time. A sampling error will be made with respect to the real HW/LW. The sampling error might be important, but no further investigations are performed on this matter in this thesis.

Only a few years of hourly observations were available for Helgoland (Fig. 4.9) and high and low waters can not be used to calculate a reliable timeseries for surge. The comparison of the descriptions of observed and modeled surge is therefore not performed.

To sum up, the trends based on the ABE simulations are all closer to the observed for Helgoland. The high waters are closer to the observed ones on a yearly basis, however, low waters are positively biased in the ABE experiment.

4.4.1.3 Borkum

The third tide gauge used for comparing long-term observations with the hindcasts is the tide gauge Borkum situated on the East Frisian island with the same name. The available hourly observations and model values are converted to values for HW/LW the same way as for Cuxhaven and used to make yearly statistics of the high and low waters. However, observation record for Borkum is only 16 years compared to 44 for Cuxhaven and 39 for Helgoland.

In Fig. 4.22 annual mean high (anMHW) and low water (anMLW), tidal range (anMTR) and upper and lover percentiles from observations and the ABE and CTL simulation are compared. The low waters are better described in the model for Borkum than Cuxhaven and the Fig 4.22 looks relatively similar to Fig. 4.21 for Helgoland. However, the modeled high waters are more than 60 cm too high on average.

The average value of high waters is 4 cm lower and towards the observed average after nudging, but this is barely visible in Fig. 4.22 because of the large bias. Studies done with another model with a higher resolution for the German Bight have not experienced the same problem with too high anMHW in the modeled experiments (Weisse pers. comm. 2005), and this indicates that Borkum might be a geographical location were the bathymetry used in the model setup is not able to reproduce values close to the observed ones at Borkum.

The large difference between the observed and modeled values of anMHW is also reflected in the anMHW made of summer and winter values for Borkum (not shown). Model values for Borkum generally differ from the observed values, which was also seen in Sec. 4.3. Not shown values of a tide-only simulation also produce higher values for the modeled sea level height than the observed for Borkum. The reason for the large bias in modeled high waters is likely due to shortcomings of the model, probably due to a poor description of the topography or the local tide. It can be concluded that ABE generally improves the CTL experiment for Borkum, but the modeled high waters differ from the observed. This large difference is most likely due to local constraints for Borkum in the model setup and it can not be expected that the nudging method should repair these modeling constraints.

Weisse and Plüß (2005) pointed out that the calculation of trends depends on their analysis period; for example for selected locations along the coast of the German Bight trends based on hindcasts and calculated from 1958-1993 were considerably larger than respective trends calculated for the period

1958-2002. They also presented a simulated timeseries from a coastal point in the German Bight having a decrease in the 90th percentile of high waters in the 1990's. As the analysis period for Borkum in this thesis starts in 1985 the negative trend observed for the high percentiles in Fig. 4.22 is supported by the study from Weisse and Plüß (2005).

All modeled trends are considerably smaller than the observed and none of the modeled trends are significant at a 95% level. On the other hand it is important to note that the observation record for Borkum is only 16 years long.

In the following the effect of nudging for surge values is investigated. Percentiles of the modeled surge at Borkum presented in Fig. 4.23 are generally too low for the CTL experiment. However, the fit after nudging is considerably improved, especially for the year-to-year fluctuations. Some deviations from the percentiles calculated from observations can be found for the lowest percentiles. The trends calculated from observations are negative for the high percentiles. However, all trends are reasonably small (about -7 to +11 cm/100 years) and in addition the analysis period for Borkum is only 16 years. In other words the trends are very sensitive for small differences between the experiments and observations for the calculated surge, and none of the calculated trends from the observations are significantly different from zero at a 0.95 significance level.

As for Cuxhaven, the differences between the different percentiles from ABE and CTL are shown in Fig. 4.24. All the high percentiles are higher in the nudged experiment, and the lower percentiles are lower. Similar features were also seen at Cuxhaven in Fig. 4.20. The visual inspection of Fig. 4.19 and Fig. 4.23 shows a mainly equal fit for surge as for Cuxhaven, but the range of the calculated surge is greater for Cuxhaven than for Borkum.

Generally the high percentiles in the difference between the ABE and CTL experiments have a negative trend (Fig. 4.24, right), and opposite for the low percentiles. But none of the trends are significant.

The Briers score for Borkum is shown in Tab. 4.2 for the different percentiles. For Cuxhaven the score is as always positive, between 0.10 and 0.76, indicating an improvement in the ABE experiment from the CTL experiment. The value for the calculated Brier score for all 44 years of modeled surge, and not just the selected percentiles, was 0.90 for Borkum in Sec. 4.3 (Fig. 4.11).

Many of the same features as for Cuxhaven and Helgoland are also seen for Borkum. The modeled high waters are better after nudging but the bias in

the modeled high water is larger than for Cuxhaven and Helgoland. The modeled surge in the inter-annual variability better is after nudging and the Brier scores improve by 10-76% for the percentiles of surge which are investigated.

As a summary of the comparison of model values with observations for long-term changes, the calculated trends from CTL, ABE and observations for the different parameters and for the tide gauges investigated in this section are given in Tab. 4.3.

	Borkum					
	99th	95th	90th	10th	5th	1st
Brier score:	0.10	0.57	0.69	0.76	0.72	0.46

Table 4.2: Brier score for percentiles of surge at Borkum. Calculated for ABE versus CTL in Fig. 4.23 with the surge calculated from observed values as the common predictand.

Trends									
Cuxhaven (1958-2001)									
	Yearly			Winter			Summer		
	CTL	ABE	OBS	CTL	ABE	OBS	CTL	ABE	OBS
anMHW	10.24	14.33	25.53	10.58	24.89	30.96	6.52	7.17	19.95
anMLW	2.65	-0.33	-5.93	4.14	6.90	9.02	-0.63	-4.64	0.13
anMTR	7.72	14.66	31.39	8.98	20.23	21.94	7.22	11.88	19.93
99%	11.52	35.30	21.54	88.06	116.52	148.50	8.52	8.82	42.68
95%	14.90	30.04	29.63	35.34	69.45	62.78	5.50	5.10	21.93
90%	15.06	22.07	32.51	24.98	44.74	59.99	5.04	5.87	18.34
10%	-1.07	-8.57	-12.97	-6.50	-16.17	-24.79	-3.15	-1.17	0.66
5%	-8.73	-10.86	-20.43	-13.26	-24.17	-35.69	-5.03	-6.28	-2.04
1%	-3.08	-8.98	-17.51	-25.90	-33.47	-53.37	-6.83	-7.39	-0.24
	Helgoland (1958-1996)						Borkum (1985-2001)		
	Yearly						Yearly		
	CTL	ABE	OBS				CTL	ABE	OBS
anMHW	7.86	13.13	33.30				5.41	6.28	27.15
anMLW	3.51	-2.55	-8.85				-3.01	-3.30	-33.14
anMTR	4.42	15.66	42.07				8.54	9.68	61.35
99%	-1.47	18.69	45.07				10.73	13.99	-64.22
95%	15.89	26.00	51.95				1.48	3.22	-43.60
90%	12.28	22.25	44.50				2.25	3.84	-14.19
10%	-3.29	-12.55	-18.26				1.09	-0.41	23.56
5%	-6.60	-15.13	-22.53				-0.62	0.28	28.02
1%	-6.22	-11.87	-13.59				-0.29	1.02	49.04

Table 4.3: Trends for the tide gauges from simulated and observed values. The analysis periods are listed in parentheses. Red values are trends trends significantly different from zero at a 95% confidence level.

4.4.2 Trends of extremes for the North Sea

Along the North Sea coast much of the hinterland (especially in the Netherlands, Denmark and Germany) is below or slightly above mean sea level and has to be protected from extremes in water level. In these countries there has always been a great interest in possible changes in water level and storm-related variations (surge) and their long-term changes.

In Sec. 4.4.1 an improvement in describing the trends for high waters and surge was shown when observations from Aberdeen were nudged into the model. External processes such as external surges are included in the ABE simulation, and modeled values were closer to the observed values than for the CTL experiment. This way the natural variability from meteorological effects is described better in the model and the remaining differences from the observations are likely to come from non-meteorological effects. In the following section changes in long-term trends after nudging are presented for the entire North Sea, instead of just focusing on the selected tide gauges. The section focuses on trends of extreme values as they are most important for coastal protection and engineering (e.g., building of wind parks.), and the differences between ABE and CTL are elaborated. In Sec. 4.3 the average conditions of the 95th and 5th percentiles calculated from sea level height as well as surge were presented and in this section the long-term changes of the same percentiles are further investigated.

Trends for the North Sea calculated from the yearly 95th and 5th percentiles of sea level height and surge are shown in Fig. 4.25. The two uppermost panels show the trends calculated from the yearly percentiles of sea level height. There is a positive trend of 10-25 cm/100 years for the 95th percentile of sea level height (first row in Fig. 4.25) in the German Bight and the Danish Coast when Aberdeen is nudged. A positive trend is also observed close to the nudged tide gauge Aberdeen. Generally the largest differences from the CTL experiment are observed in the areas in which the magnitudes of the trends in ABE are largest. Most of the trends along the coast line in the ABE experiment are significantly different from the CTL experiment, except the trends for sea level height in the southern German Bight.

For the 5th percentile (second row in Fig. 4.25) only small and mainly negative trends are observed. The most negative trends are observed in the southern part of the North Sea close to the English Channel. In the German Bight small negative trends are seen, but the trends from ABE are generally not significantly different from the CTL experiment.

The last two rows of Fig. 4.25 shows the trends in the 95th and 5th yearly percentiles calculated for surge. Positive trends of 15-35 cm/100 years are observed in the ABE experiment for the German Bight for the 95th percentile (third row in Fig. 4.25). For most of the North Sea the differences in the trends after nudging are significantly different from the CTL experiment. The largest differences between ABE and CTL are seen close to the nudged tide gauge Aberdeen, in the German Bight and on the West coast of Denmark. A considerably added value for the hindcast was achieved for surge in Sec. 4.4.1 and Sec. 4.3.1 when observations from Aberdeen were combined with the model. Thus it can be concluded that the nudging technique in a cheap way can improve the description of surge in the German Bight for multi-decadal simulations and should be used.

For protection of coastal areas it is important to make good predictions of surge. Most countries around the North Sea have an operational warning system for occurring storm surges but the countries also put a lot of effort into predicting the future levels of storm surges. An increase in surge in the German Bight for the 95th percentile of 15-35 cm/100 years over the last 44 years is an important result for the planning of future constructions of coastal protection such as dikes and storm surge barriers. However, one should note that the model simulations normally have shortcomings from effects not included such as land rise, mean sea level rise or dredging.

For the trends calculated from the 5th percentile of surge (last row in Fig. 4.25) only small negative trends are observed. The largest magnitudes are in the southern North Sea but they are not significantly different from the CTL experiment.

Positive trends for the 95th percentile of 10-25 cm/100 years for sea level height and of 15-35 cm/100 years for surge in the German Bight are comparable to the trends calculated by Weisse and Plüß (2005), who studied values only for the winter season. The largest changes in trends after nudging are achieved for the 95th percentile close to Aberdeen, which is nudged in the ABE experiment, and in the German Bight and the West coast of Denmark. This result is consistent with the changes in sea level height and surge in Fig. 4.14 for the 95th percentile.

The inference about the significance of the trends is performed according to Sec. 3.2.5 with parametric t-statistics applied. The non-parametric Mann-Kendall test described in Sec. 3.2.5 with and without pre-whiting was also tested. However, a visual inspection revealed only negligible difference in the significant areas plotted in Fig. 4.25. For this reason the same method was also used to calculate the significance of the trends used for comparing long-term observations with model results in Sec. 4.4.1.

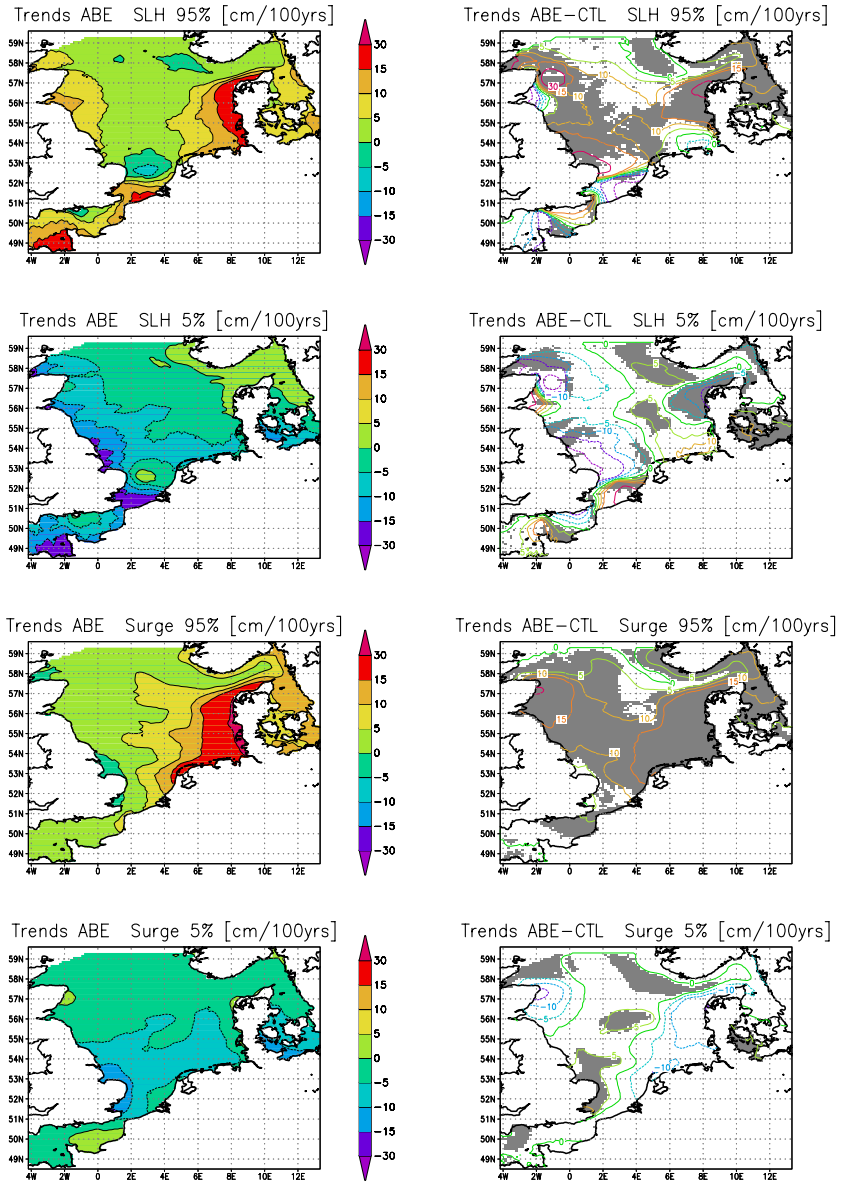

Figure 4.25: Trends for the North Sea calculated from the yearly 95th and 5th percentiles.
Left column: Trends of the 95th and 5th percentiles calculated from ABE experiment.
Right column: Trends of difference between percentiles calculated from ABE and CTL experiments. Grey areas are significantly different from zero at a 95% confidence level.
The first two rows represent SLH and the last two surge. The color interval is the same for all plots.

In Sec. 4.1 it was concluded that the model's capability of modeling the sea level height in the English Channel with the present setup is limited. For this reason the trends and differences from nudging observations from Aberdeen, located on the Northeast coast of the UK, are not discussed further for the English Channel.

4.4.3 Section summary

Extremes and trends from long-term observations from the German tide gauges Cuxhaven, Helgoland and Borkum were compared with the same statistics from a hindcast including only meteorological forcings and a hindcast utilizing long-term observations from Aberdeen together with the meteorological forcings. By nudging observations from Aberdeen into the model, external processes are taken into account. Thus, it is possible to quantify changes in the long-term variations caused by non-meteorological effects from the remaining differences between the ABE experiment and the observations. Such effects could be changes in the bathymetry by e.g. construction works (e.g. dredging, embankments) or natural morphodynamical processes, a rise in mean sea level or land rising/sinking.

A considerable improvement is achieved after nudging. Percentiles were calculated from the modeled surge and compared to observed surge for the two tide gauges Cuxhaven and Borkum in the German Bight. A visual inspection showed an improvement after nudging and according to the calculated Brier scores the percentiles of surge improved by 10-80%. This improvement is due to external effects included in the observations from Aberdeen, which are not included in the control simulation, and can be described as an improved description of the meteorology included in the model.

A seasonal cycle is seen in the quality of the simulated high and low waters, in which the modeled values for high waters are best reproduced for the winter. Even though biases in sea level height exist, the long-term trends for high and low waters mainly improve after nudging for the different tide gauges and the analysis periods.

An improved two dimensional presentation of the calculated long-term trends are presented for the North Sea. The largest changes in trends after nudging are achieved close to Aberdeen, which is nudged in the ABE experiment, and in the German Bight and at the West coast of Denmark. In the latter areas, positive trends for the yearly 95th percentile of 10-25 cm/100 years for sea level height and of 15-35 cm/100 years for surge are achieved. The trend for the 95th percentile of surge in the ABE experiment is for most of the

North Sea, significantly different from the trend in the control experiment, in which no nudging was applied. In the German Bight a small negative trend is calculated for the 5th percentile in the ABE experiment but this trend is not significantly different from the respective one in CTL experiment.

Chapter 5

Conclusion and outlook

A simple and cost-efficient nudging scheme is implemented into a North Sea version of the regional Ocean Model TRIMGEO and tested. The scheme is well suited for multi-decadal simulations and has been used for a hindcast from January 1958 to November 2001. Improved statistics for the 44 years time period were achieved. Compared to a control simulation that did not combine observations of sea level height with the model, the simulation of near-coastal sea level elevations is considerably improved for high waters. For surge, an improvement was found for both high and low surges.

The nudging method, in which external forcings are additionally taken into account, provides a considerable improvement in reproducing long-term variations and trends. Thus, it is possible to quantify changes in the long-term variations caused by non-meteorological effects from the remaining differences between the nudged experiment and the observations. Such effects could be changes in the bathymetry by e.g. construction works (e.g. dredging, embankments) or natural morphodynamical processes, a rise in mean sea level or land rising/sinking.

Observations of sea level height for the UK tide gauge Aberdeen were nudged into the model, and the RMS of modeled sea level height was reduced by 30-60% for tide gauges in the German Bight and in Norway. For surge, a considerable reduction of 70-80% is achieved for the German Bight. Generally the long-term fluctuations and biases of extreme values of high waters in the nudged simulation are considerably improved after nudging, but there is a higher bias in the description of low waters. The closer investigated tide gauges in the German Bight improve for surge values by 10%-80% for the high and low percentiles. The long-term trends for the 95th percentile

calculated from surge in the ABE experiment are significantly different from the corresponding trends from the CTL experiment for most parts of the North Sea. The largest differences are seen in the German Bight and at the West coast of Denmark. In this area positive trends of 15-30 cm/100 years are calculated for the ABE experiment. In the CTL and ABE experiment the calculated trends result from the meteorological forcings, however, with external processes included in the ABE experiment through nudging of observed sea level height from Aberdeen. Thus, the modeled variability is increased, and the modeled long-term variability and changes in the ABE experiment are generally closer to the observed values.

Presently a large variety of more or less sophisticated techniques exists for data-driven modeling. In ocean modeling so far, all efforts have focused on the simulation of relatively short periods up to a couple of years. The nudging scheme proposed in this thesis represents a relatively simple and cost-efficient option to combine long-term observations with modeling. While it may not compete with more advanced techniques for short integration periods, it represents a choice for long-term simulations as the additional computing resources required are marginal.

While a number of options exist regarding the variables and the sources of data used for data-driven modeling in short-term integrations, additional constraints apply for multi-decadal hindcasts. In particular the data used should be available on multi-decadal time scales, should have sufficient accuracy and sufficient homogeneity on multi-decadal time scales, and should be available at high spatial and temporal resolution. This thesis is therefore limited to the combination of long-term observations from coastal tide gauges that represent one of the best options to meet those requirements.

It was found that the storm surge variability in the inner model domain away from the open boundaries was reasonably well reproduced. Close to the open boundaries the storm surge variability is systematically underestimated. When observational data were nudged into the model this situation improved considerably, especially near the north-western part of the open boundary where the data have been nudged. Near the eastern part close to the Norwegian tide gauges the situation remained almost unchanged while in the inner domain an improvement was also found for the German tide gauges. This result is probably caused by a combination of boundary effects and external processes not accounted for in the control simulation. Boundary effects may comprise artificially limited fetches near the open boundary and may be particularly important in the vicinity of the boundary. Unaccounted external processes involve, for instance, so-called external surges.

In addition to nudging, an equally plausible alternative to improve the boundary values would have been to comprise an enlargement of the model domain so that boundary effects become less important in the North Sea and that external processes are more reasonably captured. As another alternative, an extra North Atlantic model could be used to provide boundary values for a multi-decadal simulation. While such a setup is optimal for operational purposes it may reach its limits for multi-decadal simulations, especially when particularly high resolutions are required near the coast. In this case nudging provides an option to reduce boundary effects and to take those processes into account that are unresolved due to the smaller model domain. It is shown in this thesis that the nudging scheme is a good alternative to extra Atlantic Models calculating the boundary conditions or the nudging scheme can be used to adjust possible disorders in the boundary conditions inside the model area.

Nudging of data from one or more British tide gauges into the model significantly improved the statistics of the simulated storm surge. The improvement is most obvious for the German tide gauges and negligible for the Norwegian ones. Most improvement was obtained already when only data from one British tide gauge have been nudged, and nudging of additional British tide gauges had only minor effects. This finding may have two important consequences for operational storm surge modeling: First, when data from a tide gauge as upstream as possible are nudged, the largest improvement for most of the coastal areas can be expected. In addition, the lead time for warnings would be largest. Second, if data from a particular tide gauge are sometimes not available in real-time, this tide gauge can be replaced by another one without having major consequences on the quality of the expected results. These findings and reasonably good availability of measurements from the British tide gauge Aberdeen motivated the hindcast from 1958 to 2001 in which Aberdeen was nudged. The Aberdeen tide gauge is located in the docks area of Aberdeen and possible local constructional works affecting the measured water level can not be excluded in the observed values. However, the long-term variations of the 90th, 95th and 99th percentile showed no trend and the impact of possible local constructional works for Aberdeen is assumed marginal for the long-term variations and trends calculated in the ABE experiment.

The investigation of the hindcasts revealed a summer/winter dependency in the differences between the modeled and observed sea level heights. For the German Bight a combination of effects was listed to explain this seasonality, however, closer investigations revealed that the seasonal differences also existed close to the northern open boundary. It is speculated that a seasonality exists in the boundary values and creates most of the seasonal differences in

modeled water levels for the German Bight. In the control run, the boundary values supply a better fit of the observations in the winter months than in the summer months. In the nudged simulation, the fit is improved for high water, especially for the summer months. As a result, generally long-term means and trends of high waters are improved after nudging while a higher bias is achieved for low waters.

Weisse and Plüß (2005) investigated the long-term storm surge variability and presented an update of, and a comparison, to the analysis performed by Langenberg et al. (1999). A high resolution regional ocean model was used and observational data from Aberdeen were combined with model data. In this thesis the sensitivity of the method to combine observations with modeling was investigated, and the choice of nudging long-term observations from Aberdeen was justified. The effects of the method on extremes and long-term changes were systematically investigated and a large added value, especially for surge, by applying nudging was concluded in this thesis.

In the control simulation a seasonality in the difference between modeled and observed water level was seen close to the northern open boundary. An interesting test for the future would have been to further investigate this feature, or possibly use another set of boundary values to describe the tide.

An interesting extension of the model setup would have been a higher resolution for the numerical model, especially for the German Bight. This could reveal if problems in modeling the water levels could be corrected by a better resolved bathymetry. Results from the finite element model, which is applied in Weisse and Plüß (2005) with a higher resolved bathymetry for the German Bight and the same meteorological forcing as in this thesis used, report no problems in reproducing the water levels for the tide gauge Borkum. A higher resolved bathymetry may also improve a quantification of non-meteorological effects for the long-term variations of sea level height and surge.

In this thesis the boundary values are prescribed without any rise in mean sea level. Such a rise would create even larger variability in sea level height and surges, than presented in this thesis. When introducing long-term observed values for the tide gauge Aberdeen, the long-term mean probably would have been a better estimator for the tide gauge's OD. Alternatively one could have applied the original level for OD at Aberdeen, which was not known at the beginning of the work. Both approaches could possibly improve the ABE experiment performed in this thesis.

The reason for Cromer being a poorer choice than Aberdeen and Whitby to nudge is a matter which should be a subject of further investigation. No

plausible explanations were found in this study, but a closer investigation of timeseries for tide gauges for which Cromer is nudged could reveal possible explanations.

While this study represents one of the first efforts to systematically assess the effect of combining models with observations in long-term simulations, recently more comprehensive efforts have been established. For instance within the ENACT project [1], funded by the European Union, a 3D variational data assimilation with the aim of producing a global ocean analysis over a multi-decadal period will be developed for the ocean model of Max Planck Institute for Meteorology (MPIM) in Hamburg.

In this thesis a very simple nudging method has been used. Already this method has provided promising results for the North Sea. Additionally, the nudging scheme applied in this thesis is one of the most cost-effective methods one can apply for combining observations with a numerical model. In the near future the nudging scheme will possibly be included in another version of the regional ocean model TRIMGEO to be used in further research for the North Sea.

[1] Enhanced ocean data assimilation and climate prediction

Acknowledgments

I would like to thank Prof. Dr. Hans von Storch for giving me the chance to prepare this thesis at the GKSS Research Centre in Geesthacht. Without his help I would not have been able to do a PhD and at the same time experience Hamburg and Germany.

Special thanks to Dr. Ralf Weisse, who was the tutor I worked closest with, and his knowledge and valuable discussions were very much appreciated. Thanks also to Dr. Saskia Esselborn for help with setting up the numerical model and together with Katja Woth helping me when problems occurred.

I am grateful for all help from the staff at GKSS research centre. Dr. Hermann Kuhn, Dr. Jens Meywerk and Dr. Hartmut Kapitza for technical help and Dr. Iris Grabeman, Dr. Dieter Eppel, Dr. Jens Kappenberg and Dr. Ulrich Callies for valuable discussions in the daily coffee sessions. I will thank Dr. Dennis Bray for help with the written English in the thesis and Jörg Winterfeldt for reading through the thesis. Discussions with other PhD and master students at GKSS research centre were also much appreciated.

Finally I would like to thank my family, my friends in Norway and in Germany, especially Doris Grundei who helped me reading through the thesis, as well as The Norwegian community in Hamburg. You all gave me moral support and were always there for me.

References

Allen, J., M. Eknes, and G. Evensen, 2000: An ensemble Kalman filter with a complex marine ecosystem model: hindcasting phytoplankton in the Cretan Sea. *Annuales Geophysicae*, **20**, 1–13.

Anderson, D., J. Sheinbaum, and K. Haines, 1996: Data assimilation in ocean models. *Rep. Prog. Phys*, **59**, 1209–1206.

Aspelien, T. and R. Weisse, 2005: Assimilation of sea level observations for multi-decadal regional ocean model simulations for the North Sea. Technical Report 2, GKSS.

Bennett, A. and P. McIntosh, 1982: Open ocean modeling as an inverse problem: Tidal theory. *J. Phys. Oceanogr.*, **12**, 1004–1018.

Bergthorsson, P. and B. Doos, 1955: Numerical weather map analysis. *Tellus*, **7**, 329–340.

Bertino, L., G. Evensen, and H. Wackernagel, 2003: Sequential data assimilation techniques in oceanography. *Int. Stat. Rev.*, **71**, 223–241.

Bjerknes, V., 1911: *Dynamic Meteorology and Hydrography Part II. Kinematics*. Carnegie Institute, Gibson Bros.

Brasseur, P., J. Ballabrera-Poy, and J. Veron, 1999: Assimilation of altimetric data in the mid-latitude oceans using the Singular Evolutive Extended Kalman filter with an eddy-resolving, primitive equation model. *Journal of Marine System*, **22**, 269–294.

Bratseth, A., 1986: Statistical interpolation by means of successive corrections. *Tellus*, **38A**.

Brink, K. and A. Robinson, editors, 1998: *The Sea, The Global Coastal Ocean*, volume 10, chapter 20. John Wiley & Sons, pages 541–594.

Cañizares, R., H. Madsen, H. Jensen, and H. Vested, 2001: Development in operational shelf sea modelling in Danish waters. *Eustarine, Coastal and Shelf Science*, **53**, 595–605.

Casulli, V. and E. Cattani, 1994: Stability, accuracy and efficency of a semi-implicit method for a three-dimensional shallow water flow. *Computers Math. Applic.*, **27**, 99–112.

Casulli, V. and G. Stelling, 1998: Numerical simulation of 3D quasi-hydrostatic, free-surface flows. *J. Hydraulic Engineering*, **124**, 678–698.

Charney, J., R. Fjortoft, and J. von Neumann, 1950: Numerical integration of the barotropic vorticity equation. *Tellus*, **2**, 237–254.

Daley, R., 1991: *Atmospheric Data Analysis*. Cambridge University Press, 3rd edition.

d'Hieres, G. C. and C. L. Provost, 1978: Atlas des composantes harmoniques de la marée dans la manche. Les annales hydrographiques 6.

Dick, S., E. Kleine, S. Müller-Navarra, H. Klein, and H. Komo, 2001: The operational circulation model of BSH bshcmod. Technical report, BSH.

Evensen, G., 1992: Using the Extended Kalman filter with a multilayer quasi-geostrophic ocean model. *J. Geophys. Res.*, **97**, 17,905–17,924.

—, 1993: Open boundary conditions for the Extended Kalman filter with a quasi-geostrophic ocean model. *J. Geophys. Res.*, **98**, 16,529–16,546.

—, 1994a: Inverse methods and data assimilation in nonlinear ocean models. *Physica D*, **77**, 108–129.

—, 1994b: Sequential data assimilation with a nonlinear quasi-geostrophic model using Monte Carlo methods to forecast error statistics. *J. Geophys. Res.*, **99**, 10,143–10,161.

Feser, F., R. Weisse, and H. von Storch, 2001: Multi-decadal atmospheric modeling for Europe yields multi-purpose data. *Eos Transactions*, **82**.

Flather, R. and J. Smith, 1998: First estimates of changes in extreme storm surge elevations due to the doubling of CO_2. *Global Atmos. Oc. System*, **6**, 193–208.

Flather, R., J. Smith, J. Richards, C. Bell, and D. Blackman, 1998: Direct estimates of extreme storm surge elevations from a 40-year numerical model simulation and from observations. *Global Atmos. Oc. System*, **6**, 165–176.

Gelb, A., 1974: *Applied Optimal Estimation*. The M.I.T. Press.

Gilchrist, B. and G. Cressman, 1954: An experiment in objective analysis. *Tellus*, **8**.

Gönnert, G., 2003: Sturmfluten und Windstau in der Deutschen Bucht Charakter, Veränderungen und Maximalerte im 20. Jahrhundert. *Die Küste*, **67**, 185–365.

Haugen, V. and G. Evensen, 2002: Assimilation of SLA and SST into an OGCM for the Indian Ocean. *Ocean Dynamics*, **52**, 133–151.

Heemink, A., K. Bolding, and M. Verlaan, 1997: Storm surge forecasting using Kalman filtering. *J. Meteor. Soc. Japan*, **75**, 305–318.

Heemink, A. and H. Kloosterhuis, 1990: Data assimilation for non-linear tidal models. *International Journal for Numerical Methods in Fluids*, **11**, 1097–1112.

Høyer, J. and O. Andersen, 2003: Improved description of sea level in the North Sea. *J. Geophys. Res.*, **108**.

Huthnance, J. M., 1997: North sea interaction with the North Atlantic ocean. *German J. Hydrol.*, **49**, 153–162.

Jazwinski, A., 1970: *Stochastic Processes and Filtering Theory*. Academic Press.

Jensen, J., H.-E. Mügge, and G. Visscher, 1988: Untersuchungen zur Wasserstandsentwicklung in der Deutschen Bucht. *Die Küste*, **47**, 135–161.

Johannesen, J., L. Røed, O. Johannessen, G. Evensen, B. Hackett, L. Pettersson, P. Haugan, and S. Sandven, 1993: Monitoring and modeling of the marine coastal environment. *Photogrammetric Engineering & Remote Sensing*, **59**, 351–361.

Kalman, R., 1960: A new approach to linear filtering and prediction problems. *Journal of Basic Engineering*, 35–44.

Kalnay, E., M. Kanamitsu, R. Kistler, W. Collins, D. Deaven, L. Gandin, M. Iredell, S. Saha, G. White, J. Woollen, Y. Zhu, M. Chelliah, W. Ebisuzaki, W. Higgins, J. Janowiak, K. Mo, C. Ropelewski, J. Wang, A. Leetmaa, R. Reynolds, R. Jenne, and D. Joseph, 1996: The NCEP/NCAR reanalysis project. *Bull. Am. Meteorol. Soc.*, **77**, 437–471.

Kauker, F. and H. Langenberg, 2000: Two models for the climate change related development of sea levels in the North Sea - A comparison. *Climate Res.*, **15**, 61–67.

Keppenne, C. and M. Rienecker, 2003: Assimilation of temperature into an isopycnal ocean general circulation model using a parallel Ensemble Kalman filter. *Journal of Marine System*, **40**, 363–380.

Koopmann, G., 1962: Die Sturmflut am 16./17. Februar 1962 in ozeano graphischer Sicht. *Die Küste*, **2**, 55–68.

Kulkarni, A. and H. von Storch, 1995: Monte Carlo experiments on the effect of serial correlation on the Mann-Kendall test of trend. *Meteorologische Zeitschrift*, **4**, 82–85.

Langenberg, H., A. Pfizenmayer, H. von Storch, and J. Sündermann, 1999: Storm-related sea level variations along the North Sea coast: Natural variability and anthropogenic change. *Cont. Shelf. Res.*, **19**, 821–842.

Loewe, P., G. Becker, U. Brockmann, A. Frohse, K. Herklotz, H. Klein, and A. Schulz, 2003: Nordsee und Deutsche Bucht 2002. Technical Report 33, BSH.

Lowe, J., J. Gregory, and R. Flather, 2001: Changes in the occurrence of storm surges around the United Kingdom under a future climate scenario using a dynamic storm surge model driven by the Hadley Centre climate models. *Climate Dyn.*, **18**, 179–188.

Mesinger, F. and A. Arakawa, 1976: Numerical methods used in atmospheric models. Technical report, Global Atmospheric Research Programme.

Ministerium für ländliche Räume, Landesplanung, Landwirtschaft und Tourismus des Landes Schleswig Holstein, 2001: Generalplan Küstenschutz - Integriertes Küstenschutzmanagement in Schleswig-Holstein. `http://www.schleswig-holstein.de/landsh/mlr/kuestenschutz/`.

OSPAR Commision, 2000: Quality status report 2000 for the greater north sea. `http://www.ospar.org/`.

Pugh, D., 1987: *Tides, Surges, and Mean Sea-level*. John Wiley & Sons.

Richardson, L., 1922: *Weather Prediction by Numerical Process*. Cambridge University Press.

Schrumm, C., 2001: Regionalization of climate change for the North Sea and Baltic Sea. *Climate Res.*, **18**, 31–37.

Siefert, W., 1970: Die Tideverhältnisse seit 1786 in der Elbe. *Deutsche Gewässerkundl. Mitteilungen*.

Soulsby, R., 1997: *Dynamics of marine sands*. Thomas Telford Publications.

Sündermann, J., S. Beddig, G. Radach, and H. Schlünzen, 2002: The north sea - problems and research needs. Technical report, Centre for Marine and Climate Research of the University of Hamburg.

UNESCO, 2003: The integrated, strategic design plan for the coastal ocean observations module of the global ocean observing system. Technical report, GOOS Report no 125.

von Storch, H., 1995: Misuses of statistical analysis in climate research. In H. von Storch and A. Navarra, editors, *Analysis of Climate Variability: Applications of Statistical Techniques*. Springer-Verlag.

von Storch, H., H. Langenberg, and F. Feser, 2000: A spectral nudging technique for dynamical downscaling purposes. *Mon. Wea. Rev.*, **128**, 3664–3673.

von Storch, H. and H. Reichardt, 1997: A scenario of storm surge statistics for the German Bight at the expected time of double atmospheric carbon dioxide concentration. *J. Climate*, **10**, 2653–2662.

von Storch, H. and F. Zwiers, 1999: *Statistical Analysis in Climate Research*. Cambridge University Press.

Wakelin, S., P. Woodworth, R. Flather, and J. Williams, 2003: Sea-level dependence on the NAO over the NW European Continental Shelf. *Geophys. Res. Lett.*, **30**, 1403, doi:10.1029/2003GL017041.

Waldron, K., J. Paegle, and J. Horel, 1996: Sensitivity of a spectrally filtered and nudged limited-area model to outer model options. *Mon. Wea. Rev.*, **124**, 529–547.

Weisse, R. and F. Feser, 2003: Evaluation of a method to reduce uncertainty in wind hindcasts performed with regional atmosphere models. *Coastal Engineering*, **48**, 211–225.

Weisse, R., F. Feser, and H. Günther, 2003: Wind- und Seegangsklimatologie 1958-2001 für die südliche Nordsee basierend auf Modellrechnungen. Technical report, GKSS.

Weisse, R. and A. Plüß, 2005: Storm-related sea level variations along the North Sea coast as simulated by a high-resolution model 1958-2002. *Submitted to Ocean Dynamics*.

Wolf, J. and R. Flather, 2005: Modelling waves and surges during the 1953 storm. *Phil. Trans. R. Soc. A*, **363**, 1359–1375.

Woodworth, P. and D. Blackman, 2002: Changes in extreme high waters at Liverpool since 1768. *Int. J. Climatol.*, **22**, 697–714.

Woth, K., R. Weisse, and H. von Storch, 2005: Dynamical modeling of North Sea storm surge extremes under climate change conditions - an ensemble study. Technical Report 1, GKSS.

Yue, S., P. Pilon, and B. Phinney, 2003: Canadian streamflow trend detection: Impacts of serial and cross-correlation. *Hydrological Sciences-Journal-des-Sciences Hydrologiques*, **48**, 51–63.

Zhang, A., B. Parker, and E. Wei, 2002: Assimilation of water level data into a coastal hydrodynamic model by an adjoint optimal technique. *Cont. Shelf. Res.*, **22**, 1909–1934.

List of Figures

List of Tables

List of Abbreviations

Abbreviation	Explanation
ABE	Aberdeen experiment (Tab. 3.1)
anMHW	Annual mean high water
anMLW	Annual mean low water
anMTR	Annual mean tidal range
BAW	German Federal Waterways Engineering and Research Institute
BODC	British Oceanographic Data Centre
BSH	German Federal Maritime and Hydrographic Agency
CCDAS	Carbon Cycle Data Assimilation System
CD	Chart Datum
CRO	Cromer experiment (Tab. 3.1)
CTL	Control experiment
DJF	December, January and February
DMI	Danmarks Meteorologiske Institut
ECCO	Estimating the Circulation and Climate of the Ocean
ENACT	Enhanced ocean data assimilation and climate prediction
ENIAC	Electronic Numerical Integrator And Computer
GIP	Generalized inverse problem
GMES	Global Monitoring for Environment and Security
GTS	Global Telecommunication System
HW	High water
LW	Low water
JJA	June, July and August
MARNET	Marines Umweltmessnetz in Nord- und Ostsee des BSH
MAWS	Marine Automatic Weather Station
MERSEA	Marine Environment and Security for the European Area
MPIM	Max Planck Institute for Meteorology
NAO	North Atlantic Oscillation
NCEP	National Centers for Environmental Prediction
N6U	Nudging experiment (Tab. 3.1)
N69	Nudging experiment (Tab. 3.1)
N65	Nudging experiment (Tab. 3.1)
N3U	Nudging experiment (Tab. 3.1)
N39	Nudging experiment (Tab. 3.1)
N35	Nudging experiment (Tab. 3.1)
OBS	Observations
OD	Ordnance datum
OSPAR	Oslo-Paris convention

QQ	Quantile-Quantiles
RMS	Root mean square error
RRSQRT	Reduced Rank Square Root filter
SEEK	Singular Evolutive Extended Kalman filter
SLH	Sea level height
SST	Sea surface temperature
suMHW	Summer mean high water
suMLW	Summer mean low water
suMTR	Summer mean tidal range
TOPEX/POSEIDON	The Ocean Topography Experiment
TRIMGEO	Tidal Residual and Intertidal Mudflat model with geographical coordinates
UK	United Kingdom
UNESCO	United Nations Educational, Scientific and Cultural Organization
WHI	Whitby experiment (Tab. 3.1)
wiMHW	Winter mean high water
wiMLW	Winter mean low water
wiMTR	Winter mean tidal range
WMO	World Meteorological Organization